# Functional analysis

# of

# estrogen and estrogen receptors

# in myoregeneration

（筋再生過程でのエストロゲンおよびエストロゲン受容体の機能の解析）

**The United Graduate School of Veterinary Science**

**Yamaguchi University**

**RATTANATRAI CHAIYASING**

**March 2022**

# CONTENTS

## ABBREVIATION LIST

| | |
|---|---|
| ANOVA | Analysis of variance |
| CSA | Cross-sectional area |
| CTX | Cardiotoxin |
| D | Days |
| DMSO | Dimethyl sulfoxide |
| E2 | 17β-estradiol |
| ER | Estrogen receptor |
| ERs | Estrogen receptors |
| ERα | Estrogen receptor alpha |
| ERβ | Estrogen receptor beta |
| ERα KO | Estrogen receptor alpha knockout |
| ERβ KO | Estrogen receptor beta knockout |
| GAPDH | Glyceraldehyde 3-phosphate dehydrogenase |
| HE | Hematoxylin and eosin |
| IGF-1 | Insulin-like growth factor-1 |
| IGF-1R | Insulin-like growth factor-1 receptor |
| NBF | Neutral buffer formalin |
| OVX | Ovariectomized |
| PCR | Polymerase chain reaction |
| PDGFRα | Platelet-derived growth factor receptor alpha |
| SD | Standard deviation |
| TA | Tibialis anterior |
| WT | Wild type |

# GENERAL INTRODUCTION

Estrogen is a type of sex steroid hormone that mainly regulates the reproductive system function in females, there are several types of estrogen, especially estradiol (E2: 17β-estradiol) is predominant in serum and important in estrogenic activity during reproductive age than other types (Luine, 2014; Nelson and Bulun, 2001). Which is a major produced by the ovaries, has been shown to maintain the function of the locomotor system is also known as the musculoskeletal system (Brown *et al*., 2008; Chidi-Ogbolu and Baar, 2019; Ikeda *et al*., 2019; Kosir *et al*., 2015). Evidence, accumulated more than decades, shows that estrogen is profoundly involved in the maintaining of locomotive organs instance of bones and skeletal muscles (Greising *et al*., 2011; McCormick *et al*., 2004; Messier *et al*., 2011). Estrogen is well known to inhibit the activity of osteoblast-mediated osteoclast and functions as a modulator in the homeostasis of bone formation (Koike *et al*., 2015). Together with bone resorption, estrogen insufficiency also affects to loss of muscle mass in qualitative and quantitative.

The low level of estrogen status in post-menopausal women or surgical removal of the ovaries by ovariectomized (OVX) affects not only the function of reproductive systems but also the function of non-reproductive systems, especially obesity, osteoporosis, and induction to occur sarcopenia (Ikeda *et al*., 2019; La Colla *et al*., 2015; Maher *et al*., 2010; Muramatsu and Inoue, 2000; Nilsson and Gustafsson, 2011). Until now, several studies report that estrogen deficiency impairs muscle regeneration after muscle tissue injury (Collins *et al*., 2019; Kitajima and Ono, 2016; McHale *et al*., 2012). The low level of estrogen has been advised to disturb the homeostasis of skeletal muscle stem cells (satellite cells) and impair skeletal muscle regeneration after skeletal muscle damage (Collins *et al*., 2019). In addition, satellite cells at the quiescent stage return to the activation stage after induced by muscle injury that shows low efficiency at a low estrogen state (Enns and Tiidus, 2008). Several reports suggested that

estrogen administration is necessary to maintain the function of musculoskeletal systems in women after menopause (Geraci *et al*., 2021; Pöllänen *et al*., 2011; Tiidus *et al*., 2013). Therefore, estrogen administration is one of the treatments to repair muscle function after frailty (Greising *et al*., 2009; Le *et al*., 2018).

The function of estrogen is regulated via two receptors, estrogen receptor (ER) α and ERβ (Baltgalvis *et al*., 2010; Diel, 2014; Ekenros *et al*., 2017; Gorres *et al*., 2011; Kalbe *et al*., 2007), and the reports indicated that mouse skeletal muscle expressed both types of ER (Milanesi *et al*., 2008, 2009). The difference between the two types of ERs in the muscle regeneration process remains unclear. Recently, it has been reported that estrogen and ERα are important to protect apoptosis in satellite cells (Collins *et al.,* 2019). Contrarily, ERβ knockout (KO) mice delayed muscle regeneration after muscle injury in the acute phase, possibly owing to increased apoptosis and diminished proliferation of satellite cells (Seko *et al.*, 2020). Hence, both ERs involve in muscle regeneration, however the present study was not spatulated which ER has a predominant effect on myoregeneration (Brown *et al*., 2009b; Diel, 2014).

Furthermore, estrogen is involved in the regulation of adipogenesis following muscle regeneration (Contreras-Shannon *et al*., 2006; Girousse *et al*., 2019; McHale *et al*., 2012; Nagai *et al*., 2018). In a low estrogen status, the accumulation of adipocytes was increased in skeletal muscle tissue (Campbell and Febbraio, 2001; Hausman *et al*., 2014; Jackson *et al*., 2013; Kiens, 2006). Nonetheless, the effect of ERs in the intermuscular adipogenesis process remain unknown.

The overall aim of this thesis to elucidate function of estrogen and ERs in myoregeneration and intermuscular adipogenesis to compare between ERα and ERβ. Which ER is an influential factor in promoting myoregeneration and inhibiting adipogenesis.

In Chapter 1, evaluation of morphological change in the process of myoregeneration in low estrogen status (OVX) mice and investigated changes in ER protein levels after OVX and

muscle injury induced by injection of cardiotoxin (CTX). Furthermore, by regularly administering estrogen to OVX mice injected with CTX, the improvement and promotion levels of morphological in muscle repair were analyzed.

In Chapter 2, morphological comparison in ERα KO and ERβ KO mice were demonstrated to investigate the effect on myoregeneration and adipose tissue formation. Chemically induced muscle damage by CTX in ER KO mice with low estrogen status. In addition, to clarify the difference in myoregeneration and adipogenesis process between both types of ER.

# Chapter 1

# Functional analysis of estrogen and estrogen receptors in skeletal muscle regeneration process

# INTRODUCTION

Estrogen, which is major produced by the ovaries, has been shown to act an essential factor in the maintenance of locomotive function (Brown *et al*., 2008; Chidi-Ogbolu and Baar, 2019; Ikeda *et al*., 2019; Kosir *et al*., 2015) as well as the regulation of reproductive organ function (Nelson and Bulun, 2001). It has long been thought that estrogen is deeply involved in the regulation of locomotive organs (such as bones and skeletal muscles) (Greising *et al*., 2011; McCormick *et al*., 2004; Messier *et al*., 2011). It is well known that estrogen suppresses osteoblast-mediated osteoclast activation and functions as a factor in the maintenance of bone mass (Koike *et al*., 2015). As well as bone loss, estrogen deficiency also induces qualitative and quantitative loss of muscle mass, a condition known as sarcopenia or frailty.

Estrogen function is exerted through two receptors, ERα and ERβ (Baltgalvis *et al*., 2010; Diel, 2014; Ekenros *et al*., 2017; Gorres *et al*., 2011; Kalbe *et al*., 2007), and it has been shown that both types of ER are distributed in mouse skeletal muscle (Milanesi *et al*., 2008, 2009). Estrogen deficiency has been suggested to interfere with the maintenance of satellite cells (skeletal muscle stem cells) and delay skeletal muscle repair after skeletal muscle injury (Collins *et al*., 2019). Additionally, muscle injury-induced activation of satellite cells is less effective at a low level of estrogen (Enns and Tiidus, 2008). It has been proposed that estrogen administration is important for maintaining musculoskeletal function in menopause women (Geraci *et al*., 2021; Pöllänen *et al*., 2011; Tiidus *et al*., 2013). Thus, estrogen administration is expected to improve muscle function and its activity (Greising *et al*., 2009; Le *et al*., 2018). Therefore, better understanding of the distribution of ERs in muscle tissue is thought to indicate that estrogen exerts some function in each process of proliferation, differentiation, and regeneration of skeletal muscle cells.

In the present study, the function of estrogen and ERs in the process of myoregeneration were clarified. For that purpose, morphologically examined the process of myoregeneration in low estrogen status (OVX) mice and investigated changes in ER protein levels after OVX and muscle injury induced by injection of CTX. Furthermore, by regularly administering estrogen to OVX mice injected with CTX, morphologically analyzed the improvement and promotion levels of muscle repair and attempted to evaluate the function of estrogen in the myoregeneration process.

## MATERIALS AND METHODS

### *Animal husbandry and ethical approval*

Adult female C57BL/6JJcl mice were obtained from CLEA Japan (Tokyo, Japan) at 6 weeks of age, weighting approximately 18−20 g body weights for experimental myoregeneration in a low estrogen status. Additionally, adult female mice (C57BL/6) for experimental myoregeneration after estrogen administration were obtained by self-mating at 6 weeks of age, weighting approximately 20−23 g body weights. The present study was focused only on female mice to avoid sex-specific differences in muscle regeneration in male mice (McHale *et al*., 2012)

Mice were housed during the experiment in the Experimental Animal Facility of Tottori University, Japan. In case of mice, their obtained from CLEA Japan were divided 4 mice in each cage (small size) and kept for two weeks to be acclimated to the facility before experiments. While mice were obtained by self-mating at 3 weeks old of age after weaning, the mice were separated from parent and kept in same cage (large size) until 6 weeks of age. Then, to divide mice into small size cage in each cage contained 3 mice and kept until experiment.

All of the mice were housed in plastic cages supplied with sawdust floor and maintained under a temperature-controlled (23 ± 1.0 °C) room condition with a 12-hr light/12-hr dark cycle. The mice were freely fed food (CLEA Rodent Diet CE-2, CLEA Japan) and water. The animal care and experimental design were approved by the Animal Research Committee, Tottori University, Japan (approval number 18-T-37).

### *Creation of low estrogen status mice*

Low estrogen status mice were created by OVX. Anesthesia was prepared as a mixture of 0.06 ml medetomidine (Dorbene 10 mg; Kyoritsu Seiyaku, Tokyo, Japan), 0.16 ml

midazolam (Dormicum 10 mg; Maruishi, Osaka, Japan) and 0.2 ml butorphanol (Vetorphale 5mg; Meiji Seika, Tokyo, Japan), and up to 1 ml normal saline (0.9% NaCl; Otsuka Pharmaceutical, Tokushima, Japan) (Kawai *et al*., 2011). Mice were weighed using a digital scale ELT-402 (Sartorius, Gottingen, Germany). Anesthesia was intraperitoneally administered [0.005 ml/g body weight] to female mice (8 weeks old) using a 27 g × 3/4" needle (Terumo, Tokyo, Japan). Aseptic technique was used to clean the lateral aspect of the body of mice. Lateral incision was made to open abdominal cavity via a blunt puncture through the abdominal wall. The ovary was pulled out of the abdominal cavity and dissected. Then, to return the fat pad and tissue into abdominal cavity and repeated the process on the opposite side. The skin was closed with wound clips (Autoclip 9 mm; Becton Dickinson and Company, Sparks, MD, USA). Antidote of anesthetic agents was prepared as mixture of atipamezole 0.12 ml (Atipame 5 mg: Kyoritsu Seiyaku, Tokyo, Japan), and up to 1 ml normal saline (Otsuka Pharmaceutical). Antidote was intraperitoneally injected [0.005 ml/g body weight] to OVX mice for restore sedative mice return to normal state. After that mouse were kept on a heating pad at approximately 38 °C to maintain body temperature until full recovery. Post-operative mice were held overnight for critical care. Then, 7 days after operation, surgical wound was inspected once daily. Incision wound clips (Becton Dickinson and Company) were removed 7−10 days after sugery.

***Confirmation of low estrogen level***

To confirm the low estrogen level of OVX mice, intact female mice (controls, 8 weeks old) and the mice at 4 weeks after OVX treatment (12 weeks old) were anesthetized and blood was collected by tail laceration. The blood was immediately centrifuged for 10 min and serum was collected. The collected serum was frozen and stored at −30 °C until use. Serum estradiol (E2) levels were measured by an enzyme-linked immunosorbent assay (Cayman Chemical,

Ann Arbor, MI, USA), in accordance with the manufacturer's protocol. The linear equation of standard curve was created to determine serum estradiol level (ng/ml). The experiment was conducted after confirming that serum E2 concentration in OVX mice was significantly lower than that in intact mice.

***Experimental myoregeneration in low estrogen status***

Mice were divided into two groups (n = 16 in each group). The first group at 4 weeks after OVX treatment, 50 μl of 10 μM CTX from *Naja pallida* (Latoxan, Portes lès Valence, France) was injected at the middle belly part of the right tibialis anterior (TA) muscles of OVX mice (C57BL/6JJcl) using a syringe with an injection needle (29G 1/2 insulin syringe, Nippon Becton Dickinson and Company, Fukushima, Japan) (OVX/CTX group). The second group was intact mice were not treated with OVX and were injected with CTX (Intact/CTX group). In each group, TA muscles were sampled on 3, 7, 10 and 14 days after CTX injection (D3, D7, D10 and D14) (n = 4 at each time point). The left TA muscle on D3 was analyzed as a non-injured (control) group. All mice were sacrificed by cervical dislocation under anesthesia with isoflurane (MSD Animal Health, Osaka, Japan). The collected TA muscles were divided into two parts: 1) the proximal part was used for ER protein analysis (Western blotting) and was kept at −80 °C until use and 2) the distal part was fixed with 10% neutral buffer formalin (NBF; Wako, Osaka, Japan) and used for histological analysis.

***Experimental myoregeneration after estrogen administration***

Mice (C57BL/6) at 4 weeks after OVX (12 weeks of age) were injected CTX into right TA muscle and randomly divided into two groups. The first group of mice received regular E2 (Wako) dissolved in dimethyl sulfoxide (DMSO; Wako) as a vehicle and the second group of mice received only DMSO. In the first group, E2 was continuously administered

intraperitoneally every 4 days until the 28th day (D28) after CTX injection. The concentration of E2 per administration was 0.8 μg/body weight of 100 g, and it was dissolved in 50 μl DMSO (Nagai *et al*., 2016). In the second group, only the same amount of DMSO was administered each time. TA muscles on left and right legs were collected at D28. The right TA muscles injected with CTX were designated as OVX/CTX/E2 and OVX/CTX based on the respective treatments. The left TA muscles that were not injected with CTX were similarly designated as OVX/E2 and OVX. These four types of TA muscles with different treatments were fixed with 10% NBF and then analyzed histologically.

***Evaluation of myoregeneration***

The 10% NBF-fixed TA muscles were dehydrated in graded ethanol series (Wako), cleared in xylene (Wako) and embedded in paraffin. Cross-sections (6 μm in thickness) were then stained with hematoxylin and eosin (HE) for histological analysis. For evaluation of myoregeneration, five non-overlapping field were photographed, the minor axis diameters (smallest diameters) of 200 myotubes per animal (40 myotubes per field) were measured using image analysis software (ImageJ; v1.46r, National Institutes of Health, Bethesda, MD, USA). The diameter of the minor axis of myotubes per animal was measured at a magnification of 200 times (Mahdy *et al*., 2015).

***Distribution of myotube diameter***

Myofiber diameters or myotube diameters range was set up at 5 μm per interval. The rages started from 5 μm (minimum range) to 80 μm (maximum range) was showed on the X-axis of histogram graph. Number of myofibers (frequency) was showed on the Y-axis of the graph. The distribution line of a histogram created by Microsoft Excel (Microsoft, Redmond, WA, USA).

***Evaluation of muscle recovery***

Evaluation of the recovery ratio (%) of muscle injury was calculated by the average diameter of newly formed myotubes with a central nucleus in both the Intact/CTX and OVX/CTX groups was divided by the average diameter of myofibers in the non-injured group as control at each time point. The recovery ratio (%) of OVX mice for comparison with intact mice was calculated by the average diameter of myofibers or newly formed myotubes with a central nucleus divided by the average diameter in intact mice at each time point. The repair speeds (μm/day) in the first period (D7 to D10), second period (D10 to D14) and total period (D7 to D14) of CTX-injected mice were determined by the inclination is changed in average diameter of regenerated myofibers in each group was divided by the duration period of day after injury.

***Western blotting***

After TA muscle protein extraction by using a protein extraction kit (Cosmobio, Tokyo, Japan), protein concentration was determined by the bicinchoninic acid method (Thermo Fisher Scientific, Rockford, IL, USA). Proteins were electrophoresed on polyacrylamide gels (Life Technologies, Carlsbad, CA, USA) and transferred to a nitrocellulose membrane (Life Technologies). After blocking in 5% w/v non-fat dry milk for 1 hr, the membrane was incubated for 1 hr at room temperature (RT) with rabbit monoclonal anti-glyceraldehyde 3-phosphate dehydrogenase (GAPDH, 1:2000; Cell Signaling Technology, Danvers, MA, USA), rabbit polyclonal anti-ERα antibody (1:1000, Sigma, St. Louis, MO, USA), and mouse monoclonal anti-ERβ antibody (1:400, Novus Biological, Centennial, CO, USA) as the primary antibody. The membrane was washed in Tris-buffered saline with 0.1% Tween 20 (TBS-T) and incubated for 1 hr at RT with goat anti-rabbit IgG-peroxidase (1:20000 for GAPDH, 1:5000 for ERα, Sera Care Life Sciences, Milford, MA, USA) or goat anti-mouse IgG-peroxidase

(1:1000 for ERβ, R&D Systems, Minneapolis, MN, USA) as the secondary antibody. After washing five times in TBS-T and incubation in immunodetection reagent (Bio-Rad, Hercules, CA, USA), protein levels were visualized using a Western blotting image membrane scanner (LI-COR Biosciences, Lincoln, NE, USA) and densitometric values were determined with Image Studio software (ver 4.0; LI-COR Biosciences). Protein levels of ERs were calculated on the basis of GAPDH.

***Statistical analysis***

The E2 concentration in serum was analyzed by an unpaired Student's *t*-test. Histometric and ER protein intensity data were analyzed by one-way analysis of variance (ANOVA) with Bonferroni's *post-hoc* test. All data are expressed as average ± SD. Analyses were performed with Excel Statistics 2016 for Windows (ver. 3.21; SSRI, Tokyo, Japan). Statistical significance was defined as $p < 0.05$.

## RESULTS

### *Serum estrogen level in OVX mice*

Serum E2 level at 4 weeks after OVX treatment was significantly lower than that in the intact group, confirming that the OVX mice used in the myoregeneration experiment were in a low estrogen status (Fig. 1).

### *Myoregeneration in a low estrogen status*

#### *Morphological change*

On D3 after CTX injection, a large amount of cell infiltration into the muscle tissue was observed. Muscle degeneration was more severe in the OVX/CTX group than in the Intact/CTX group. On D7, new eosin-stained myofibers with a central nucleus appeared in both groups. In addition, cells with less cytoplasm, which are clearly different from myotubes, were distributed in the inter-myotube space. These newly-formed myotubes had a nearly circular cross section in mice in the Intact/CTX group, but many myotubes in mice in the OVX/CTX group showed a distorted shape rather than a circular shape. On D10, myotubes of various sizes with central nuclei were observed in both the Intact/CTX and OVX/CTX groups. On D14, the myotubes had begun to form a polygonal structure with multiple nuclei distributed around the myotubes, resembling non-injured muscles, but they still had a central nucleus. On D10 and D14, myotubes with large diameters were observed more frequently in the Intact/CTX group than in the OVX/CTX group (Fig. 2A).

#### *Comparison of myotubes diameter*

A comparison of the diameters of myofibers in intact and OVX mice in non-injured controls showed that the average value in OVX mice was slightly lower than that in intact mice,

but there was no significant difference between the two groups. On D3, the diameter of myofibers could not be measured due to collapse of the myofibers. The OVX/CTX group had smaller myotube diameters than those in the Intact/CTX group at all time points, D7, D10 and D14. Throughout the 14-day experimental period after CTX injection, the diameter of regenerated myotubes increased in both groups. However, the diameter in the OVX/CTX group was always significantly smaller than that in the Intact/CTX group throughout the experimental period. The myotube diameters at D14 were 49.1 ± 2.72 μm in the Intact/CTX group and 38.1 ± 0.39 μm in the OVX/CTX group (Fig. 2B).

***Comparison of diameter range and distribution of myotube diameters***

The distribution of myofiber diameters in non-injured ranging from 40 μm to 80 μm in intact, but in OVX mice the distribution was increased, to a minimum range of 35 μm and a maximum range of 80 μm. However, the highest number of myofibers range (highest frequency range) in OVX mice was lower than that in intact mice: 50 μm in OVX mice and 55 μm in intact mice. On D7, the distribution of myotube diameters in the OVX/CTX and Intact/CTX group had the same ranging from 15 μm to 45 μm, but the highest number of myotubes range in the OVX/CTX group was lower than that of Intact/CTX group. The values were 30 μm and 35 μm in OVX/CTX and Intact/CTX groups, respectively. The highest number of myotubes range at D10 in both groups was the same as 35 μm. Nevertheless, the cumulative number of myotubes diameters range (cumulative frequency range) in OVX/CTX group ranging from 25 μm to 30 μm was higher than that in Intact/CTX group. While the cumulative number of myotubes range in Intact/CTX group ranging from 40 μm to 50 μm was higher than that in OVX/CTX group. The distribution of myotube diameters in OVX/CTX group at D14 was lower than that in Intact/CTX group. The value ranging from 25 μm to 60 μm in OVX/CTX group and from 15 μm to 70 μm in Intact/CTX group. Moreover, the highest number of

myotubes range in OVX/CTX group was lower than that in Intact/CTX. The highest number of myotubes range at D14 were 40 μm in OVX/CTX group and 55 μm in Intact/CTX group. In the experimental period of 14 days after CTX injection, the maximum range of myotube diameters increased in both groups. However, the distribution of myotube diameters in the OVX/CTX group was lower than that in the Intact/CTX group from D10 to D14 of experimental period. In addition, a trend of the distribution line shifted to the right and close to non-injured in both groups when the day went by (Fig. 3A and B).

***Comparison of muscle recovery potential***

The ratio (%) of both group (Intact/CTX and OVX/CTX) at D14 were 91.4 ± 5.06% and 72.7 ± 0.74%, respectively, of the diameter of myotubes in the non-injured control mice. In both groups, the ratio (%) of the average diameter of myotubes to non-injured controls increased with the passage of days. However, the ratio in the OVX/CTX group was significantly lower than that in the Intact/CTX group (Fig. 4). The ratios (%) of the average diameters of myofibers and myotubes in OVX-treated mice to those in intact mice at each time point are shown in Fig 5. OVX/CTX mice showed significantly lower ratios than those in non-injured mice at all time points. In addition, the ratios on D14 in OVX/CTX mice were significantly lower than the ratios on D7 and D10. Fig. 6 shows the repair speed of regenerated myotubes during a period of 7 days (first half period: D7 to D10, second half period: D10 to D14) after CTX injection. In the first half period, there was no significant difference between the two groups, but the OVX/CTX group showed a significantly lower speed than that in the Intact/CTX group in the second half period and throughout the whole period (D7 to D14). In the second half period, the Intact/CTX group had the highest repair speed, while the OVX/CTX group had the lowest, which was about 2.26-times lower than that in the Intact/CTX group.

***Evaluation of ER proteins in a low estrogen status***

Changes in ER (ERα and ERβ) proteins after injection of CTX into OVX mice (OVX/CTX) were evaluated by Western blotting. The protein levels (band intensity ratios) of the two ERs that are reportedly distributed in skeletal muscle showed a predominance of ERβ over ERα in all samples. However, when the amounts of each receptor protein were compared in intact and OVX mice, there was no significant difference between the two groups. On D7, the samples of OVX/CTX mice showed a sharp increase in values in both ERs compared to those in intact and OVX mice. After that, the values of both ERs decreased over time, but the values of ERβ remained significantly higher at D14 than those in intact and OVX mice (Fig. 7). The intensity of the GAPDH band at D7 in OVX/CTX mice was lower than that of the other samples. In this experiment, the proteins extracted from each sample were adjusted to the same concentration (15 mg/15 ml/lane) and electrophoresis was repeated, and the same results were obtained in each case.

***Myoregeneration after estrogen administration***

Myofibers in the OVX and OVX/E2 groups, unaffected by CTX-induced muscle injury, maintained a polygonal cross-section with peripheral nuclei. On the other hand, in the OVX/CTX and OVX/CTX/E2 groups, myotubes with a central nucleus were still observed at D28 after CTX injection. In addition, most of the myotubes in the OVX/CTX group had a clearly smaller diameter than those in the other three groups (Fig. 8A). The average diameters of myofibers in the OVX and OVX/E2 groups were 56.8 ± 2.13 μm and 59.3 ± 1.09 μm, respectively, and there was no significant difference between the two groups. On the other hand, the OVX/CTX group, which had muscle injury under the condition of a low estrogen status, had a significantly low value of 48.1 ± 1.40 μm, but the diameter of myotubes in the OVX/CTX/E2 group, which was continuously administered E2, was 55.7 ± 0.85 μm. This

value was not significantly different from OVX/E2 group (Fig. 8B). The minimum range of myofiber diameters in the OVX group was lower than that in OVX/E2. The value was 35 μm in OVX group and 45 μm in OVX/E2 group, but the maximum range of myofiber diameters was the same as 80 μm. The distribution of myotube diameters in the OVX/CTX group ranging from 30 μm to 75 μm, but in OVX/CTX/E2 the distribution was decreased, to a minimum range of 40 μm and a maximum range of 80 μm. Moreover, a trend of the distribution line shifted to the left in OVX/CTX groups when compared with the other groups. While the OVX/E2 and OVX/CTX/E2 remained similar OVX group (Fig. 8C and D).

## DISCUSSION

The aim of the present study to elucidate the function of estrogen and ERs in the myoregeneration process and morphogenesis. In addition, to evaluate the morphological change after E2 administration in low estrogen status.

### *Low estrogen status delayed myoregenration*

The diameters of regenerated myotubes in OVX mice after CTX injection (OVX/CTX) were significantly smaller than those in intact mice after CTX injection (Intact/CTX) at all time points (D7, D10, and D14). McHale *et al.* (2012) also reported that cross-sectional area (CSA) of regenerated myotubes in OVX mice at 14 days after CTX injection was smaller than that in intact mice. Most of the satellite cells, which play an important role in the myoregeneration process, remain in a quiescent status in healthy or uninjured muscle tissue. However, the muscle injury caused by mechanical loading or chemical injection activates satellite cells from a quiescent state to a state of proliferation, leading to the myoregeneration process (Chargé and Rudnicki, 2004; Mann *et al*., 2011; Schmidt *et al*., 2019; Tidball, 2017; Wada *et al*., 2008). In this study, the ratio and speed of muscle repair after CTX injection differed depending on the estrogen concentration. The myoregeneration ratio was generally low in OVX mice compared to that in intact mice (Fig. 4). In addition, the ratio of myotube diameter in OVX/CTX mice to that in Intact/CTX mice was lowest at D14 (Fig. 5). The repair speed of regenerated myotubes in OVX/CTX mice was significantly slower than that in Intact/CTX mice throughout the period of D7-D14, and the decrease in speed was remarkable in the second half period (D10 to D14). Several studies have shown that estrogen is deeply involved in apoptosis avoidance and cell proliferation *via* ERs (Galluzzo *et al*., 2009; Haines *et al*., 2018, Kitajima and Ono, 2016; Seko *et al*., 2020; Velders *et al*., 2012). Therefore, estrogen deficiency is directly linked to the loss

of satellite cells (Collins *et al*., 2019). The significant difference in the second half period may be due to an insufficient number of satellite cells required to maintain a smooth myoregeneration process. The results strongly suggest that muscle injury in a low estrogen status induces satellite cell loss, followed by delayed differentiation into myoblasts, resulting in delayed myoregeneration.

***Influential of ERβ predominance than ERα in myoregenration***

Protein levels of the two ERs (ERα and ERβ) in TA muscles of mice showed a predominance of ERβ over ERα in both intact and OVX mouse samples. The expression of both ERα and ERβ has been reported in skeletal muscle in many animal species (Kalbe *et al*., 2007; Milanesi *et al*., 2008, 2009), but ERβ is thought to be the major isoform in mice (Milanesi *et al*., 2009). In this experiment, injection of CTX into OVX mice (OVX/CTX) significantly increased ERβ production at D7, followed by a gradual decrease while maintaining high levels compared to those in OVX mice. Serum E2 levels increase in the early stages of trauma in adult human patients. This phenomenon suggests that estrogen may play an important role in the protection of traumatic organs (Brown *et al*., 2009a; Groswasser, 2001). Continuous measurement of serum E2 levels after CTX injection into TA muscles of healthy (non-OVX-injection) mice showed a significant increase in E2 levels 1-10 days (peaking on the 7th day) after CTX injection and a sharp decline after the 15th day (Liao *et al*., 2019). Unfortunately, serum E2 levels in OVX mice after CTX injection were not measured in our experiments. However, it is reasonable to assume that mice lacking ovaries, the main source of E2 in the body, have low E2 levels. The reason for the increase in ERβ level in OVX/CTX mice at D7 to D14 may be the cellular response to low E2 levels in the body. It is considered that the expression of ERβ in injured muscle tissue was upregulated to maintain the signal input from E2, which has a strong impact on myoregeneration. However, when considering this result,

attention should also be paid to the OVX/CTX band intensity at D7 of the Western blot shown in Fig. 7. In the OVX/CTX tissue image of D7 in Fig. 2A, newly generated myotubes are scattered and necrotic cell/tissue fragments remain in the space between the myotubes. Also, some infiltrating cells are observed. Therefore, abundant cell/tissue fragments within regenerated muscle tissue, secreted proteins from infiltrating cells, and the extracellular matrix may have affected the intensity of the GAPDH band. It will be necessary to consider the effects of these proteins on the ER band. Further experimentation is needed to clarify the details of these remaining questions.

***E2 administration rescued muscle recovery in low estrogen status after injury***

In this study, the effect of a low E2 status on muscle recovery was investigated. In a previous study in which E2 was administered to OVX rats with hindlimb suspension-induced disuse atrophy of skeletal muscle, the soleus muscle CSA recovered as in intact rats (McClung *et al*., 2006). This suggests that estrogen is an essential factor for rescue of muscle recovery in a low E2 status. Being consistent with the results of that study found that the diameter of regenerated myotubes in CTX-injured mice continuously treated with estrogen (OVX/CTX/E2 in Fig. 8) was significantly larger than that in OVX/CTX mice. The results showed that the diameter of myofibers in OVX/E2 mice was not affected by estrogen administration. It can be said that estrogen is a factor that acts when satellite cells are in a proliferated or differentiated state after muscle damage.

In conclusion, the present study provided evidence that estrogen is an essential factor for the maintenance of satellite cell proliferation and differentiation in the smooth progression of myoregeneration. Further elucidation of the mechanism of the myoregeneration process will

enable the establishment of new strategies for maintaining female muscle function by targeting the estrogen-ERβ pathway.

## MINI SAMMARY

In the present study, functions of estrogen and ERs in the myoregeneration process and morphogenesis were elucidated, to compare their effects on the morphological change, moreover, the alteration of the ER protein level during muscle regeneration was analyzed by western blotting following muscle injury with CTX.

TA muscles of OVX adult female C57BL/6 mice were injured with CTX. Muscle degeneration was severe in OVX mice than intact mice as control at D3 after CTX injection. However, muscle regeneration started at D7 days in both OVX and intact mice, OVX mice showed poorly reconstruction than intact mice at D10 and D14, respectively. The diameter of regenerated myotubes in OVX mice was significantly smaller than that in intact mice at all time points after injury. OVX mice also showed lower muscle recovery rates and slower speeds than did intact mice. ER protein levels showed a predominance of ERβ over ERα in both intact and OVX states. The ERβ level was increased significantly at D7 after CTX injection in OVX mice and remained at a high level until D14. In addition, continuous administration of E2 to OVX mice in which muscle injury was induced resulted in a significantly larger diameter of regenerated myotubes than that in mice that did not receive estrogen.

This study provided evidence that estrogen is an essential factor in the myoregeneration process since estrogen depletion delayed myoregeneration in injured muscles and administration of estrogen under the condition of a low estrogen status rescued delayed myoregeneration. The results strongly suggested that ERβ may be a factor that promotes myoregeneration more than does ERα.

# Chapter 2

# Modulation of myoregeneration and intermuscular adipogenesis by estrogen receptors

# INTRODUCTION

Estrogen deficiency in women after menopause or OVX affects not only reproductive dysfunction but also non-reproductive functions such as sarcopenia, obesity and predisposition to develop frailty (Ikeda *et al*., 2019; La Colla *et al*., 2015; Maher *et al*., 2010; Muramatsu and Inoue, 2000; Nilsson and Gustafsson, 2011). So far, there have been several reports that low estrogen status inhibits regeneration of damaged muscle tissue (Collins *et al*., 2019; Kitajima and Ono, 2016; McHale *et al*., 2012). Skeletal muscles express estrogen receptor α (ERα) and ERβ; however, the functional difference between the two types of ERs remains unclear, especially in the morphology of muscle regeneration. Collins *et al.* (2019) reported that estrogen and muscle satellite cell expression of ERα is necessary to prevent apoptosis of satellite cells. On the other hand, Seko *et al.* (2020) insisted that ERβ knockout (KO) mice exhibited impaired muscle regeneration following acute muscle injury, probably due to reduced proliferation and increased apoptosis of satellite cells. Thus, there are several reports on the involvement of both ERs in muscle tissue regeneration, but it was not concluded which ER action has a strong effect on myoregeneration (Brown *et al*., 2009b; Diel, 2014). Moreover, estrogen has been reported to affect the regulation of adipocyte accumulation in regenerating muscle (Contreras-Shannon *et al*., 2006; Girousse *et al*., 2019; McHale *et al*., 2012; Nagai *et al*., 2018). When the estrogen concentration decreased, adipogenesis was accelerated in skeletal muscle tissue (Campbell and Febbraio, 2001; Hausman *et al*., 2014; Jackson *et al*., 2013; Kiens, 2006). However, the effect of ERs in the process of adipogenesis is poorly understood. In the current study, the CTX was chemically induced muscle damage in ER KO mice with low estrogen status and morphologically evaluated the effect of estrogen and ERs on myoregeneration and adipose tissue formation.

## MATERIALS AND METHODS

### *Animals*

Two subtypes of ERα KO and ERβ KO and wild-type (WT; C57BL/6) mice were used in this study. ERα KO mice were obtained by mating mice of a mixed C57BL/6 background that were heterozygous for ERα gene disruption, as described previously (Dupont *et al*., 2000). Ers2$^{tm1Unc}$/J, ERβ gene disruption mice were purchased from The Jackson Laboratory (Bar Harbor, MA, USA), and ERβ KO was obtained by mating mice of a mixed C57BL/6 background that were heterozygous (Hewitt *et al*., 2000; Krege *et al*., 1998). After 28 days of age, genotypes of both subtypes of ERs KO mice were determined by multiplex PCR. Female WT, ERα KO, and ERβ KO mice were used in the current study. The animal experiments were approved by the Animal Research Committee of Tottori University, Japan (approval number: 18-T-37, 32-040).

### *Animal operation and muscle injury procedure*

All mice (aged 8 weeks old) underwent OVX under anesthesia as previous described in Chapter 1. OVX mice were divided into 3 groups (n = 3): OVX-WT (control), OVX-ERα KO, and OVX-ERβ KO group. Four weeks after OVX (aged 12 weeks), tibialis anterior (TA) muscles were injected with CTX as previous described in Chapter 1. The contralateral left TA muscle was left intact and served as the non-injured control. The injured TA muscles were collected on after euthanasia on D7, D10, and D14, respectively, after CTX injection. In addition, the non-injured control (left) TA muscles were also collected at D7. All mice were sacrificed by inhalation of an overdose of isoflurane (MSD).

### *Measurement of estrogen level in serum*

E2 concentration in serum was measured as previous described in Chapter 1.

***Histological analysis***

The collected muscle tissue and the ovaries was immediately immersed in 10% neutral buffered formalin and fixed at room temperature for 16 hr. Then, a series of procedures were performed to embed the tissue in paraffin. HE-stained and Masson's trichrome-stained paraffin sections (6 μm thickness) were examined using an inverted light microscope (IX71, Olympus, Tokyo, Japan). Digital images were obtained and used to evaluate morphological changes in the ovaries and myofibers, regenerated myotube diameter, adipocyte accumulation and connective tissue deposition.

***Myoregeneration analysis***

To evaluate myogenesis, the regenerated muscle region was defined as follows: a region of newly formed myotubes with a central nucleus, residual region of necrotic myofibers, and a region of regenerated myotubes of various sizes with a central nucleus. In the myoregenerated region, we randomly selected approximately 150 myotubes (including the center region of the section) per specimen (at 200 × magnification), and the minimum diameter of myofiber was measured as the axis diameter of the fibers (Mahdy *et al*., 2015; McHale *et al*., 2012).

***Distribution of myotube diameter***

The evaluation of the distribution of myotube diameter followed the method described in Chapter 1.

***Evaluation of adipogenesis area***

Adipogenesis area (%) was defined as the area of adipocytes distributed between and among individual regenerated myotubes with central nuclei at all time points post injection or non-injured myofibers. For the adipogenesis area (%) calculation, 4 images of non-overlapping areas at 200× magnification were chosen after manual outlining of the intermuscular adipocyte area and dividing by the total area of the image using the image analysis software (ImageJ; v1.46r, National Institutes of Health, Bethesda, MD, USA) (McHale *et al*., 2012; Ochoa *et al*., 2007).

***Masson's trichrome staining***

Muscle sections were stained with Masson's trichrome stain to detect changes in tissue composition after CTX injury and quantify the areas of muscle (red), adipocytes (transparent) and connective tissue (blue). The stained sections were observed at a magnification of 200× with a light microscopy, 4 images of each section, 3 mice at each time point were randomly selected and analyzed with Image J software (National Institutes of Health). After adjusting the threshold, each area was displayed as a percentage of the total area (Mahdy *et al*., 2015).

***Assessment of skeletal muscle recovery***

Assessment method of the recovery ratio (%) and myoregeneration rate (μm/day) in OVX mice was described in Chapter 1.

***Statistical analysis***

Data were expressed as average ± SD. Obtained data were analyzed with StatView software, version 5.0 (SAS Institute, Cary, NC, USA) using Student's *t*-test, two-tailed to compare the E2 concentration in serum. One-way ANOVA followed by Bonferroni's *post-hoc* test was used to compare the histometrical data. Significance level was set as $P < 0.05$.

## RESULTS

### *Serum estrogen level in ER KO mice*

Before OVX treatment of the ERα KO group, E2 concentration in serum was particularly higher than that in the other groups. The E2 concentration in the serum of all groups (three types of OVX mice) 4 weeks after OVX treatment was significantly lower than that before treatment. For this reason, the mice used in the muscle regeneration experiment are in a "low estrogen state" (Fig. 9).

### *Morphological change in ER KO mice*

#### *Ovary*

The characteristic of ovary was a difference in ER KO mice when compared with WT mice as control. The ovary of ERα KO mice was appeared to enlarge hemorrhagic cystic in ovary. Contrary, there was no appeared in ERβ KO mice. Numerous unruptured follicles were found in ERβ KO mice (Fig. 10).

### *Myofiber and myotube*

On D7 after CTX treatment, the myofibers with a central nucleus appeared, and the start of muscle regeneration was confirmed. Moreover, adipocytes appeared between the regenerated myofibers in all mice. That is, muscle regeneration and adipocyte differentiation were observed on the same specimen on D7 (Fig. 11). Cell infiltration in connective tissue and regenerated myofibers appeared by D7 in all OVX treated mice. However, OVX-ERβ KO mice showed residual necrotic myofibers on D7. At D10, OVX-ERβ KO mice showed cell infiltration between the regenerated myofibers. Moreover, myofibers of all three types of OVX

mice on D14 appeared to be well regenerated when compared with non-injured myofibers (Fig. 12A).

***Comparison of myofibers diameter***

When comparing the diameters of myofibers of the non-injured control, there was a significant difference between each group, and the diameters of non-injured control of OVX-ERα KO mice and -ERβ KO mice were significantly smaller than those of non-injured control of OVX-WT. Moreover, when comparing the ER KO mice, OVX-ERβ KO mice showed a significantly lower value than that of OVX-ERα KO mice (Fig. 12B). Throughout the 14 days of the experimental period after CTX treatment, the diameter of newly formed myotubes increased over time in all groups. The average diameter of the myotube at D14 was OVX-WT mice: 40.2 ± 2.83 μm, OVX-ERα KO mice: 35.4 ± 2.69 μm and OVX-ERβ KO mice: 30.2 ± 2.81 μm.

***Comparison of diameter range and distribution of myotube***

The distribution range of myofiber diameters in non-injured control, there was a difference between group in a minimum rage, maximum range, and the highest number of myofibers range of OVX-ERα KO mice and OVX-ERβ KO mice was lower than those of OVX-WT. Moreover, when comparing the ER KO mice, OVX-ERβ KO mice showed lower value than that of OVX-ERα KO mice. The experimental period after injury with CTX injection from D7 to D14, the distribution line of myotube diameters shifted to the right and trended to close the non-injured in all types of mice. The maximum range of the myotube diameters at D14 was OVX-WT mice: 55 μm, OVX-ERα KO mice: 50 μm and OVX-ERβ KO mice: 45 μm (Fig. 13, 14A and 15A).

***Potential of ERs in myoregenration***

The ratio of the average diameter of myofibers in each group to non-injured control at each time point is shown in Fig. 14B. The value of OVX-ERβ KO group was significantly lower than those of OVX-WT and OVX-ERα KO group, respectively, but all values tended to increase. On the other hand, Fig. 15B shows the ratio (%) of the average diameter of myofibers in each group to the average diameter of OVX-WT mice at each time point. From D7 to D14, the value of OVX-ERα KO mice changed from 83.5 ± 1.39% to 88.0 ± 0.50%, and the value of OVX-ERβ KO mice changed from 63.6 ± 1.47% to 75.2 ± 0.42%. In both groups, their values increased with the passage of days. However, the value of OVX-ERβ KO mice was significantly lower than OVX-ERα KO mice. Fig. 16 shows the rate of increase in myofiber diameter during the 7 days (first half period: D7 to D10, second half period: D10 to D14) after injury, that is, repair speed of regenerated myofibers. At the same duration period, there was no significant difference between groups, but OVX-ERβ KO mice was higher than the other groups on first half period and OVX-ERα KO mice was higher than the other groups on second half period. Of the three groups, the OVX-ERβ KO mice indicated the highest value through the period (D7 to D14).

***Adipogenesis in OVX-ER KO mice***

Intermuscular adipocytes appeared among the regenerated myotubes in OVX mice at D7. Adipocyte differentiation was observed within the regenerated muscle in OVX mice at D14 (Fig. 17A). The adipogenesis area (%) in OVX-ERβ KO mice was the largest compared to other types at all time points. At D14, the adipogenesis area in OVX-ERβ KO mice was about 1.49 and 1.95 times higher than that in OVX-ERα KO and OVX-WT mice, respectively (Fig. 17B).

***Comparison of three compartment in muscle tissue***

Masson's trichrome staining revealed the ratio of muscle, fat and connective tissue. Connective tissue was originally present between myofibers, but in D7, the ratio (%) of connective tissue in all three types of OVX mice increased sharply compared to non-injured control. As the days went by, the ratio of connective tissue decreased with D10 and D14, and on the contrary, the ratio of fat increased. Interestingly, the ratio of muscle in each group remained almost constant regardless of the time after injury (Fig. 18).

## DISCUSSION

In the previous chapter, the results indicate that estrogen is a key factor in myoregeneration process since deletion delayed myoregeneration. The results of the evaluation of ERs protein strongly suggested that ERβ may be an influential factor that promotes myoregeneration more than does ERα. Recently, a study by Collins *et al.* (2019) reported that estrogen and ERα are necessary to maintain myoregeneartion smoothly. On the other hand, Seko *et al.* (2020) insisted that ERβ KO mice exhibited impaired muscle regeneration following acute muscle injury. Moreover, estrogen regulates adipocyte deposition in regenerating muscle, after estrogen concentration decreased, adipogenesis was accelerated in skeletal muscle tissue (McHale *et al*., 2012). Thus, the current study was searched out to insist on the effect of estrogen and ERs on myoregeneration and adipose tissue formation. The morphologically was evaluated following chemically induced muscle injury by CTX in ER KO mice with low estrogen status.

### *Low estrogen status in ER KO mice delayed myoregeneration*

In the current study, the diameter of regenerated myotubes in ER KO mice after injury in low estrogen status was measured. These value in ER KO mice was significantly smaller than that in WT mice. To maintain myofiber formation, the following steps should proceed in an orderly manner: 1) proliferation of satellite cells, 2) differentiation into myoblasts, 3) fusion myoblasts, and 4) elongation of myotubes (Forcina *et al*., 2000; Karalaki *et al*., 2009; Relaix and Zammit, 2012). However, in ER KO (both subtypes) mice, the myofiber diameter was significantly low. Satellite cells are stem cells of myofibers, and their initial cell growth is important for muscle regeneration smoothly. Several researchers mentioned that estrogen and ERs are necessary for satellite cell survival and proliferation (Collins *et al*., 2019; Kitajima and

Ono, 2016; LaBarge *et al*., 2014; Seko *et al*., 2020; Velders *et al*., 2012). If satellite cell survival and proliferation were inhibited due to low estrogen status, this experiment may imply that the low number of satellite cells at early stages reflects the delay of myoregeneration.

***ERβ play a key role in regulating myoregeneration***

The myofiber diameter was significantly smaller in ERβ KO mice than in ERα KO mice. Based on these results, it can be inferred that the action of estrogen *via* ERβ has a stronger effect on the maintenance of muscle tissue homeostasis than ERα. ERβ is thought to regulate not only satellite cell growth, but also prevent apoptosis in the differentiation steps of myofiber formation (Seko *et al*., 2020). However, ERα is thought to be involved in the maintenance of the number of satellite cells in the proliferation process (Collins *et al*., 2019). Our results indicated that the recovery ratio of ERβ KO mice was lower than that of ERα KO mice, indicating that the loss of ERβ could not accelerate myofiber formation in several steps. On the other hand, ERα KO mice showed better regeneration of myofiber formation than ERβ KO mice. Taken together, ERβ is likely to play a more important role in regulating myoregeneration than ERα in muscle tissue.

***ER regulate myoregeneration process***

A difference was observed in the muscle regeneration speed between ERα KO mice and ERβ KO mice. That is, the muscle regeneration speed of ERβ KO mice tended to be high in the first half period (D7 to D10) and that of ERα KO tended to be high in the second half period (D10 to D14). It is considered that this difference in myoregeneration rate depending in the timing after injury may reflect the functional regulation by each ER at each stage of myoregeneration process such as proliferation and differentiation of satellite cells, and myotube formation. The detail of functional regulation by ER need to be further examined.

***Absence of ER lead to intermuscular adipogenesis***

All types of OVX mice after CTX injury were significantly increased in the adipogenesis area (%) at D7, D10, and D14 after injury compared with non-injured control. OVX-ERβ KO mice showed a larger adipogenesis area (%) than OVX-ERα and OVX-WT mice. Delay of myoregeneration and induction of intermuscular adipogenesis in CTX-injured OVX-ER KO mice may alter the muscle and fat metabolism pathways and alter gene expression in muscle tissue. For example, myostatin, a member of the transforming growth factor-β superfamily, is a protein synthesized and released by myocytes that act as muscle cells to suppress myogenesis, such as muscle cell growth and differentiation (Deng *et al*., 2017; McPherron *et al*., 1997). In a previous study, myostatin inhibited intermuscular preadipocyte differentiation *in vitro* (Li *et al*., 2011; Sun *et al*., 2016). However, in a low estrogen state, muscle regeneration itself was suppressed, resulting in a decrease in muscle mass and production and expression of myostatin, which may have promoted the proliferation and differentiation of adipocytes. In contrast, it has been reported that adipocyte stimulated interleukin-6 expression in muscle cells could suppress muscle cell differentiation (Seo *et al*., 2019). Platelet-derived growth factor receptor α (PDGFRα) -positive mesenchymal progenitor cells are thought to be the origin of intermuscular adipocytes (Uezumi *et al*., 2010). In our experiments, adipocytes increased between myofibers after tissue damage, but the area of adipocytes formed varied significantly between ERα KO mice and ERβ KO mice. It is easy to imagine that the number and proliferation of PDGFRα-positive mesenchymal progenitor cells have a great influence on the proliferation of adipocytes after muscle tissue damage, but to our best knowledge, there are no reports of ER expression in PDGFRα-positive mesenchymal progenitor cells. By elucidating the relationship between ER and PDGFRα-positive mesenchymal progenitor cells, we will be able to get closer to elucidating the mechanism of ectopic adipocyte accumulation after postmenopausal muscle injury.

***Myoregeneration was maintained by several mechanisms besides estrogen-ER***

Initially, the current study aimed to clarify whether estrogen and ER affect muscle regeneration. The results of the comparison in ER KO mice revealed that ER function in myoregeneration is more important for ERβ than ERα. Also, it has been reported that estrogen and ER are important factors in the proliferation and differentiation of satellite cells (Collins *et al*., 2019; Kitajima and Ono, 2016; Seko *et al*., 2020; Velders *et al*., 2012). However, it is interesting that even in OVX-ER KO mice, in which the low estrogen status and the absence of ER, muscle regeneration was delayed. This phenomenon may indicate that there are other mechanisms besides estrogen-ER that maintain the progression of myoregeneration. Insulin-like growth factor-1 (IGF-1), which is known to be a major factor in the increase in skeletal muscle mass (Adams and McCue, 1998), and IGF-1 and its receptor (IGF-1R) appear to be linked to estrogen and ER. Temporary interruption of estrogen supply weakened ER signaling and dramatically increased IGF-1 compared to normal conditions (Iida *et al*., 2019). In addition, administration of estrogen to OVX animals suppressed IGF-1 production (Tsai *et al*., 2007). There are other cases where IGF-1 signaling is regulated by ER pathway. For example, in lung cancer cells, estrogen has been shown to elevate the IGF-1 signaling pathway *via* ERβ (Tang *et al*., 2012). In addition, there is an interaction between IGF-1R and ERα, which act synergistically to promote the proliferation of nucleus pulposus cells (Chen *et al*., 2020). However, there are still many uncertainties about the relationship between estrogen and IGF-1, and their receptors in muscle tissue. Focusing on these factors, it is necessary to elucidate the detailed mechanism of myogenesis and myoregeneration. Of course, it is quite possible that factors other than those mentioned above are involved in the formation of muscle, fat and connective tissue after muscle injury. It is also reasonable to assume that the many number of infiltrated cells observed in the connective tissue between myofibers after muscle injury

perform a variety of functions in a complex manner. Therefore, further research is needed to determine the biological significance of these cells and phenomena.

***Promising model for sarcopenia study was described by OVX mice***

In this experiment, adipose accumulation was observed in the skeletal muscle tissue of OVX mice after CTX injury (Figs. 17 and 18). Moreover, myofiber diameter and cross-sectional area of TA muscle did not recover until the CTX pre-injury level (Figs. 12, 14B and 18). In sarcopenia, accumulation of ectopic adipose tissue is observed in skeletal muscle, as well as atrophy of myofibers and deterioration of muscle strength and physical function (Ikeda *et al*., 2019; Srikanthan *et al*., 2010). Comparing the CTX-injured and sarcopenic muscle, there are many morphologically similar parts. The results has not investigated the function of CTX-injured mice, but it can be easily inferred that the muscle mass and strength of TA muscle of these mice are reduced. The mice used in this experiment may be a good model candidate for pathophysiological studies of sarcopenia.

In conclusion, our data may indicate that low estrogen affects myoregeneration *via* the ER. In addition, its action was more remarkable *via* ERβ rather than by ERα, and it was morphologically shown that removal of these ERs delayed muscle regeneration and promoted adipose tissue formation. Targeting estrogen and ER may provide clues for maintaining muscle tissue homeostasis.

## MINI SUMMARY

The current study purposed to compare the function of ERα and ERβ in a low estrogen status in the process of myoregeneration and intermuscular adipogenesis by morphometrical analysis.

OVX-ER KO mice were used to assess the effect of estrogen on the myoregeneration process. TA muscle was collected on D7, D10, and D14 after CTX injection to assess myotube morphology and adipogenesis area. Furthermore, the ratio (%) area of three compartment (muscle, adipocyte and connective tissue) were assessed. Regenerated myotubes from OVX-ERβ KO mice were consistently smaller in diameter than those from OVX-ERα KO and OVX-wild-type mice, whereas the adipogenesis area of OVX-ERβ KO mice was consistently greater than that of the other types. Moreover, connective tissue was originally appeared between muscle fibers, but in D7, the ratio (%) of connective tissue in all three types of OVX mice increased sharply compared to non-injured OVX mice as control. As the days went by, the ratio of connective tissue decreased with D10 and D14, and on the contrary, the ratio of fat increased. However, the ratio of muscle in each type of OVX mice remained almost constant regardless of the time after injury.

In summary, ERβ may be an influential factor in promoting myoregeneration and adipogenesis inhibition compared to ERα. In addition, OVX mice may be a promising model for pathophysiological studies of sarcopenia.

# Figures

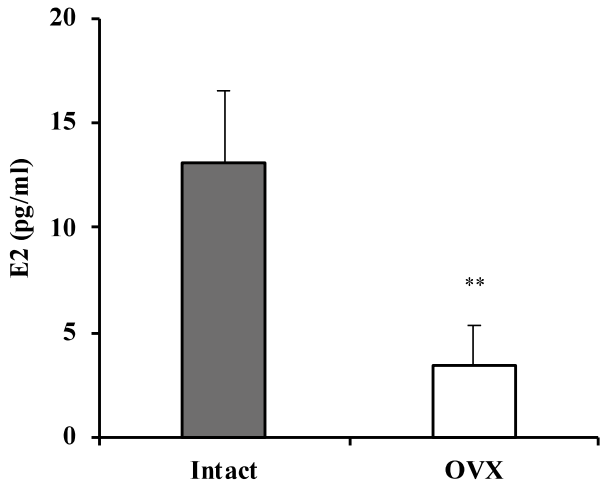


Fig. 1. Estradiol (E2) concentrations in serum of OVX mice and intact mice as controls. n = 6 in the OVX group and n = 3 in the Intact group. Data are expressed as average ± SD, ** indicates significant difference between the two group, $p < 0.01$, unpaired Student's *t*-test.

A

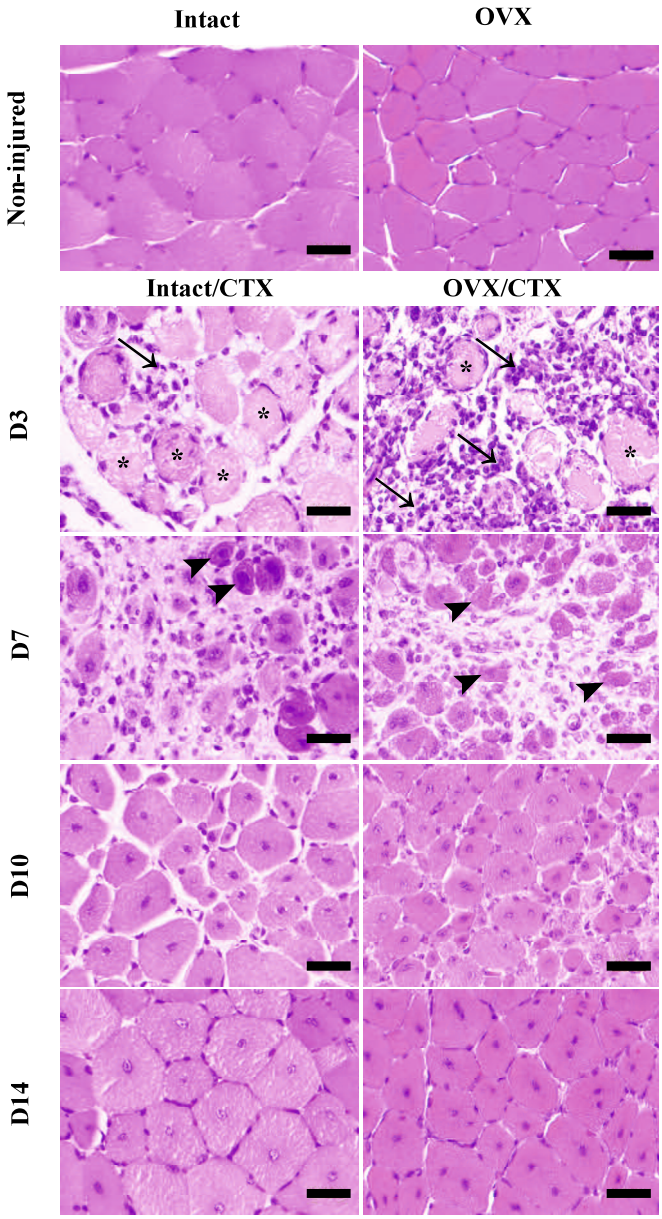
Intact
OVX
Non-injured
Intact/CTX
OVX/CTX
D3
D7
D10
D14

B

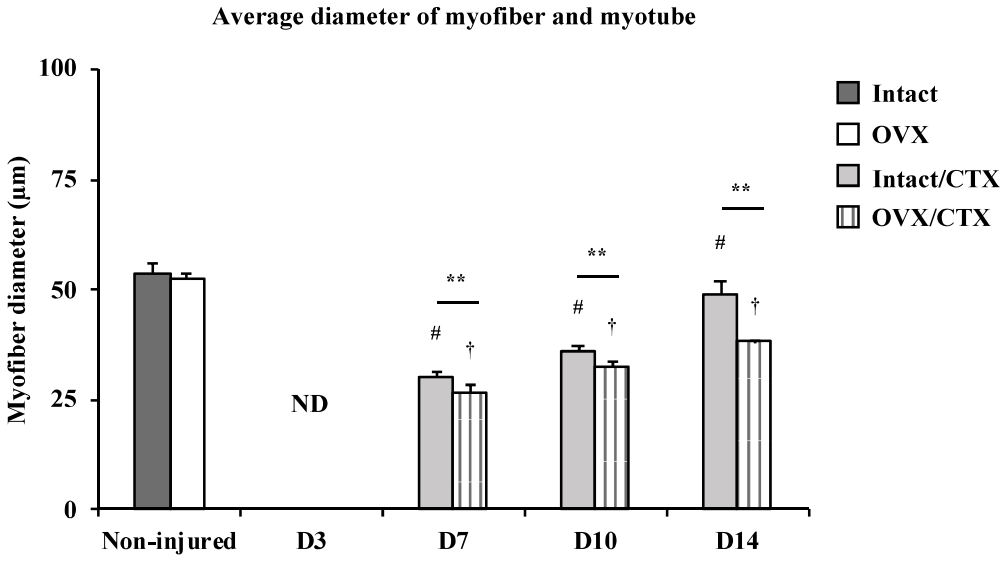
Average diameter of myofiber and myotube
Myofiber diameter (μm)
100
75
50
25
0
ND
**
#
†
Non-injured
D3
D7
D10
D14
Intact
OVX
Intact/CTX
OVX/CTX

Fig. 2. (A) Morphological changes of TA muscles in the Intact/CTX group compared with those in the OVX/CTX group at D3, D7, D10 and D14 after CTX injection. Arrows indicate cell infiltration. Asterisks and arrowheads indicate degenerated and newly-formed myotubes, respectively. Scale bar: 50 μm. (B) Comparison of the diameters of regenerated myotubes at different time points after CTX injection between the Intact/CTX group and OVX/CTX group. ** indicates significant difference between groups, # indicates significant difference from intact groups (non-injured), † indicates significant difference from OVX groups (non-injured), $p < 0.01$. ND, not detected.

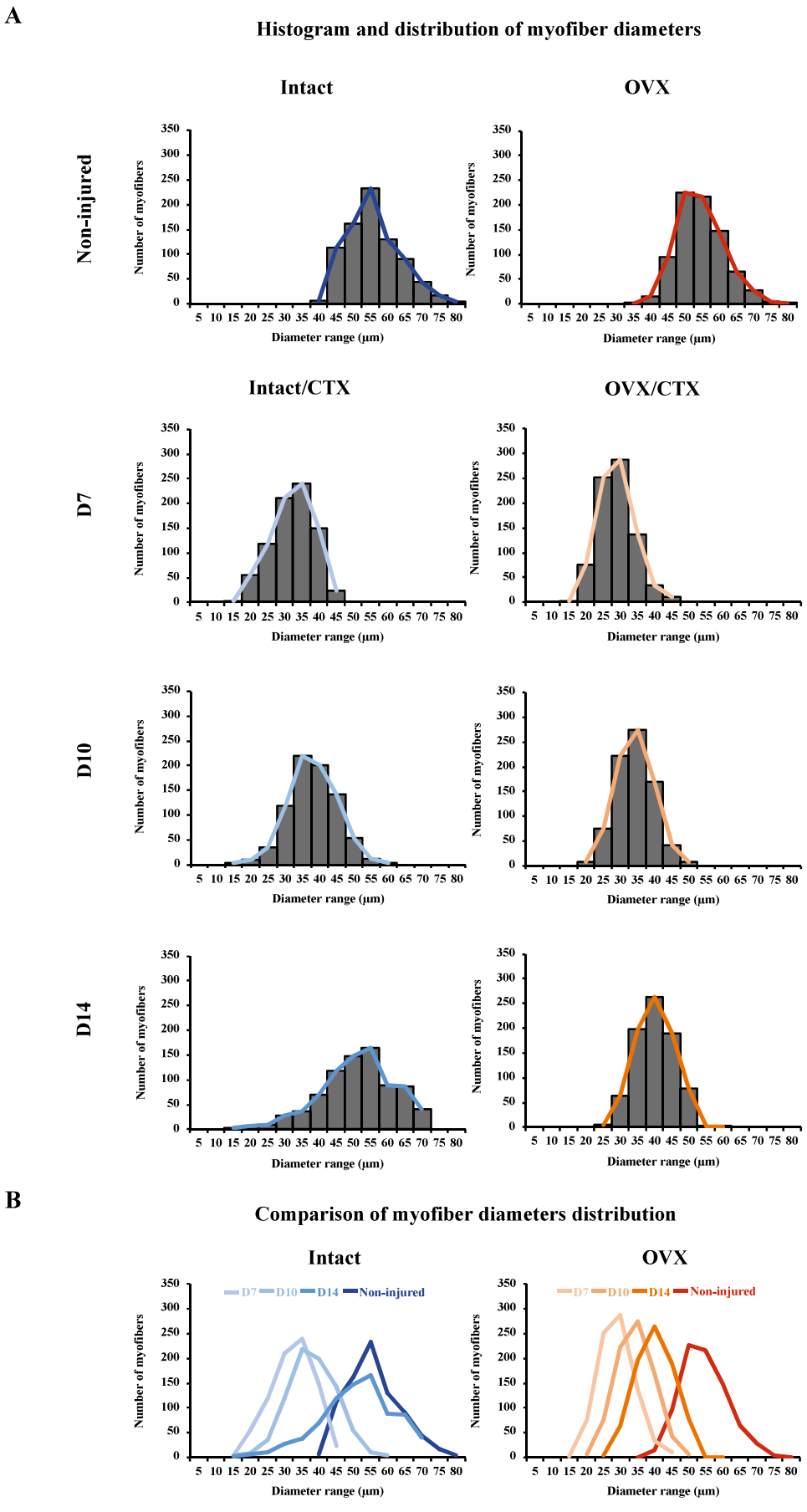
A
Histogram and distribution of myofiber diameters
Intact
OVX
Non-injured
Intact/CTX
OVX/CTX
D7
D10
D14
Number of myofibers
Diameter range (μm)
B
Comparison of myofiber diameters distribution
D7
D10
D14
Non-injured

Fig. 3. (A) Histogram of myofiber and myotube diameters in the Intact/CTX group compared with those in the OVX/CTX group at Non-injured, D7, D10 and D14 after CTX injection. (B) Comparison of the distribution line of myofiber and myotube diameters in the Intact/CTX group and OVX/CTX group at non-injured and all time points after CTX injection.

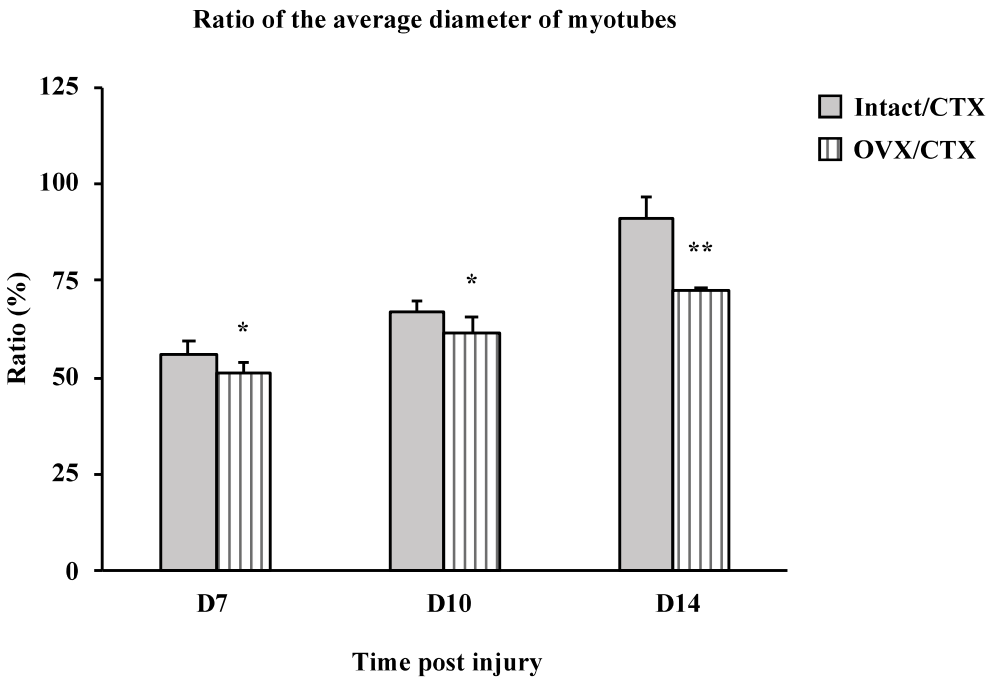


Fig. 4. Ratio (%) of the average diameter of myotubes to non-injured controls. Data are shown as average ratio ± SD. * and ** indicate significant difference from Intact/CTX mice, $p < 0.05$ and $p < 0.01$, respectively.

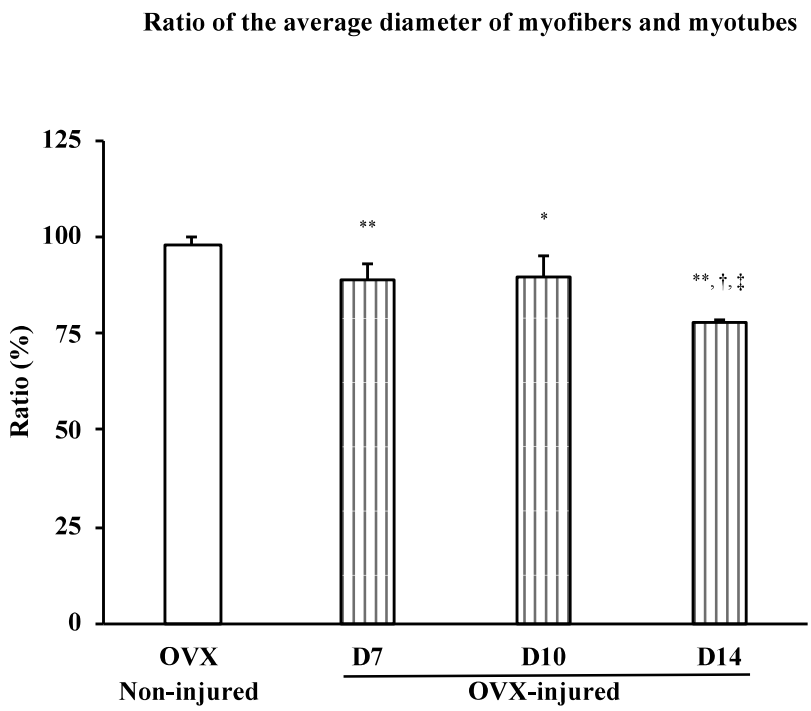


Fig. 5. Ratio (%) of the average diameter of myofibers and myotubes in OVX-treated mice to those in intact mice. Data are shown as average ratio ± SD. * and ** indicate significant difference from non-injured, $p < 0.05$ and $p < 0.01$, respectively. † and ‡ indicate significant difference from D7 and D10, respectively ($p < 0.01$).

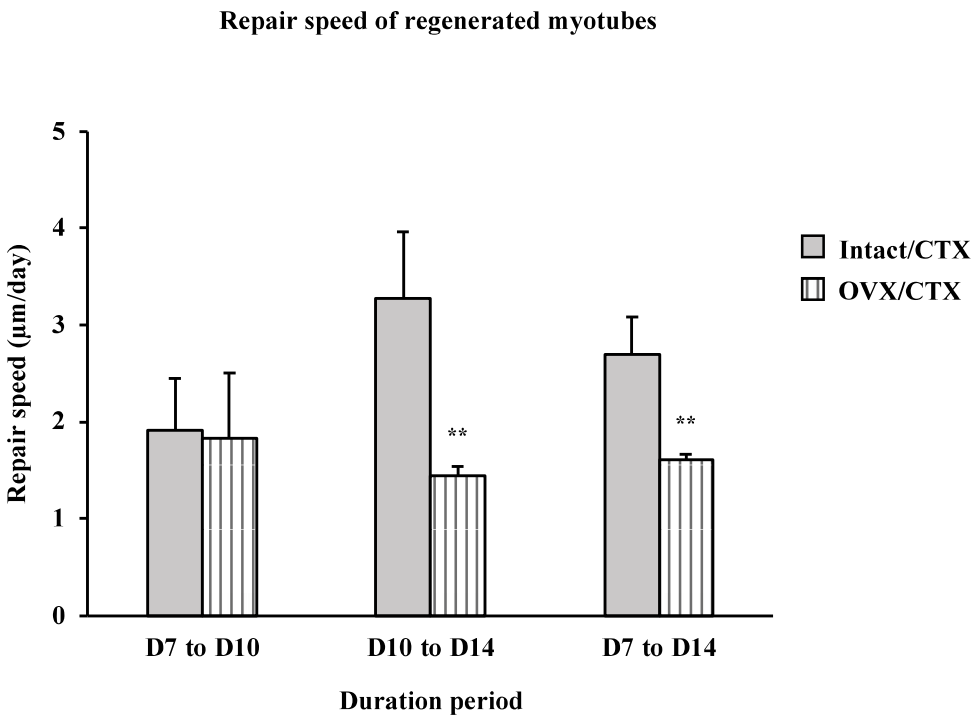


Fig.6. Repair speed (μm/day) of regenerated myotubes at several duration periods of days after CTX injury. Data are shown as repair speed ± SD. ** indicates significant difference from Intact/CTX mice, $p < 0.01$.

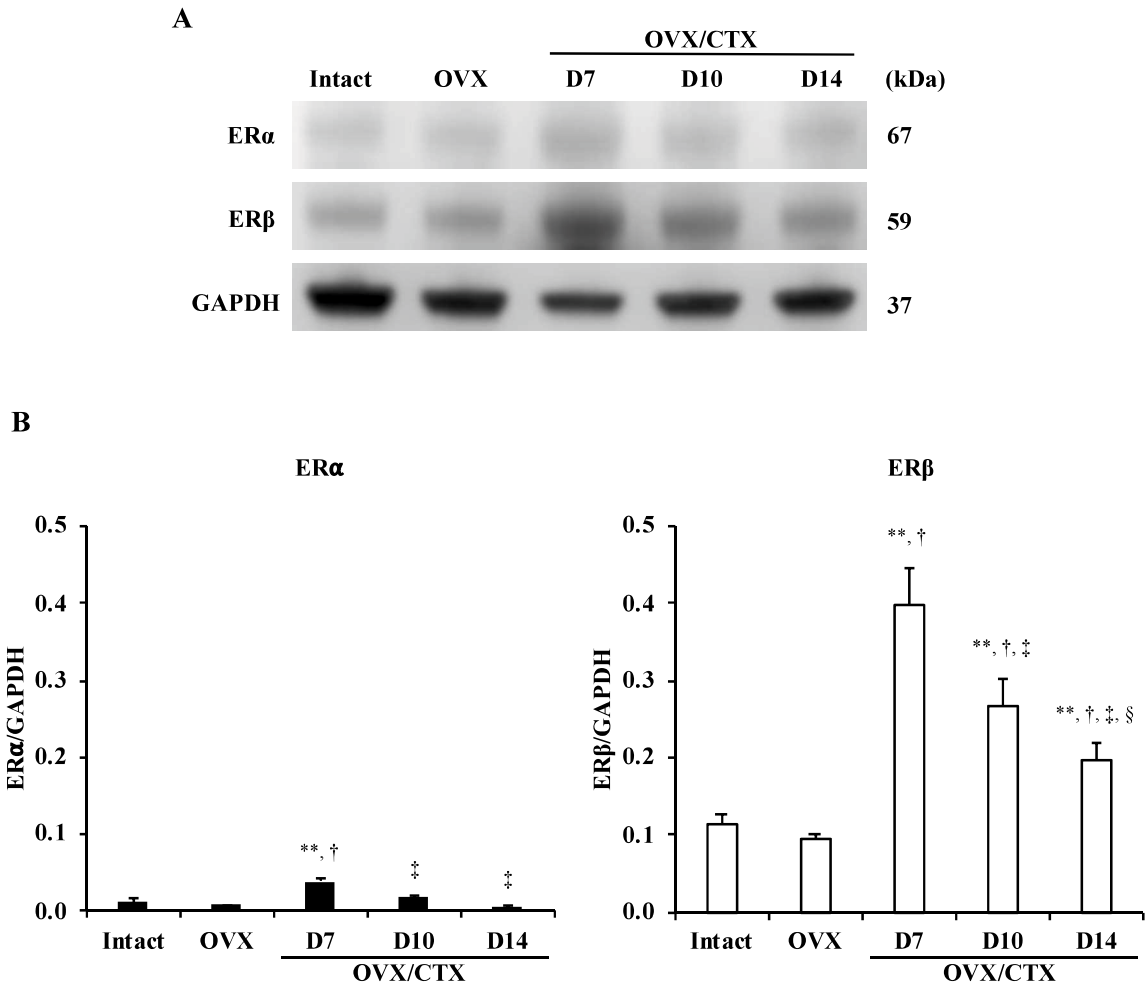


Fig. 7. (A) Western blot analysis of ERα and ERβ in the TA muscles of intact mice, OVX mice and OVX mice at D7, D10 and D14 after CTX injection (OVX/CTX). (B) Bar graph shows the band intensity ratios in ERα and ERβ. Data are expressed as average ± standard deviation, n = 3/group, **, † and ‡ indicate significant differences from intact mice, OVX mice and D7 respectively ($p < 0.01$), § indicates significant differences from D10, $p < 0.05$.

A

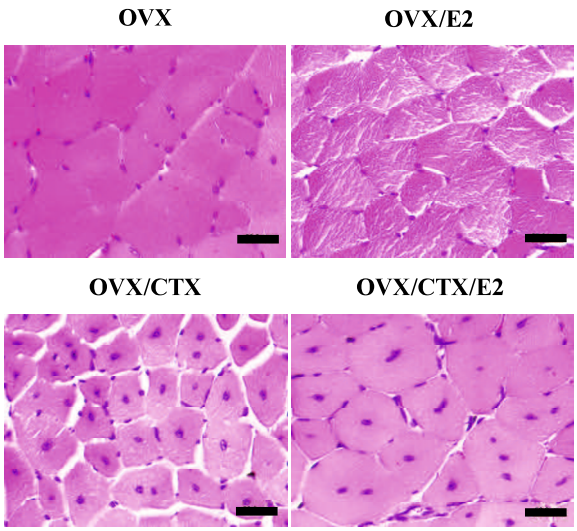
OVX
OVX/E2
OVX/CTX
OVX/CTX/E2

B

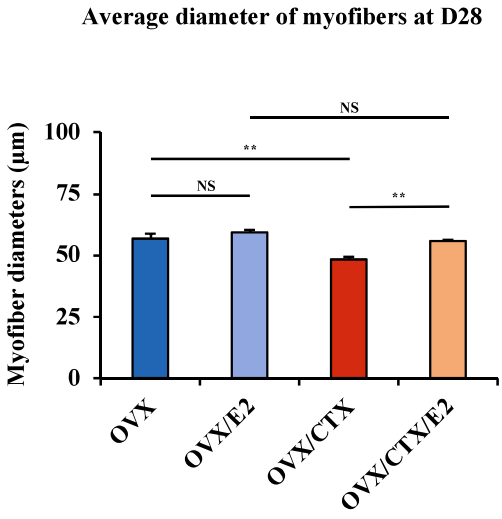
Average diameter of myofibers at D28
Myofiber diameters (µm)
100
75
50
25
0
NS
**
NS
**
OVX
OVX/E2
OVX/CTX
OVX/CTX/E2

C

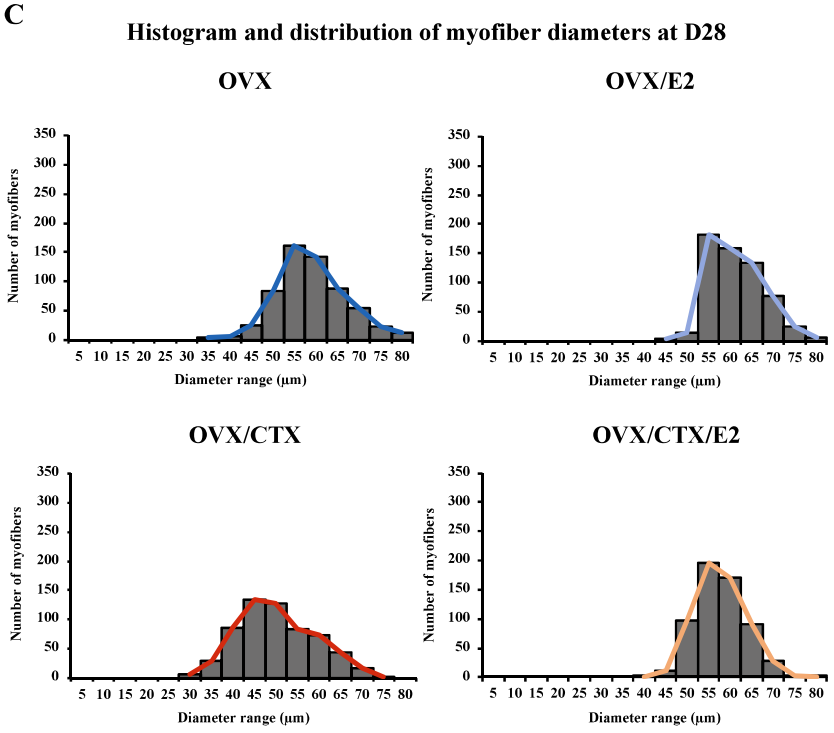
Histogram and distribution of myofiber diameters at D28
OVX
OVX/E2
OVX/CTX
OVX/CTX/E2
Number of myofibers
Diameter range (µm)
5 10 15 20 25 30 35 40 45 50 55 60 65 70 75 80
0 50 100 150 200 250 300 350

D

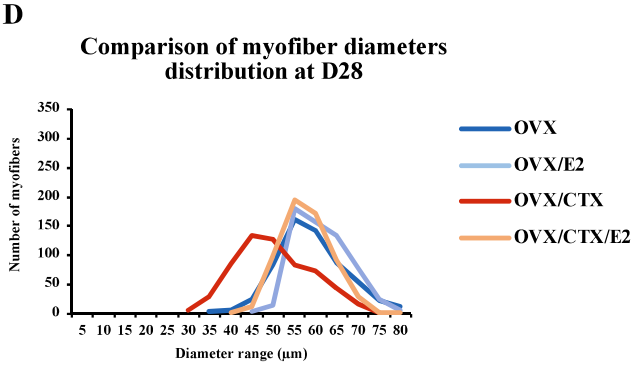
Comparison of myofiber diameters distribution at D28
Number of myofibers
Diameter range (µm)
5 10 15 20 25 30 35 40 45 50 55 60 65 70 75 80
0 50 100 150 200 250 300 350
OVX
OVX/E2
OVX/CTX
OVX/CTX/E2

Fig. 8. (A) Morphological changes of TA muscles in the OVX, OVX/E2, OVX/CTX and OVX/CTX/E2 groups at D28 after CTX injection, scale bars: 50 μm. (B) Comparison of the average diameters of myofibers and regenerated myotubes in the OVX, OVX/E2, OVX/CTX and OVX/CTX/E2 groups. Data are expressed as average ± SD, ** indicates significant difference between groups, $p < 0.01$. NS, not significant. (C) Histogram and distribution of myofiber and myotube diameters in four groups of mice. (D) Comparison of the distribution line of myofiber and myotube diameters between groups.

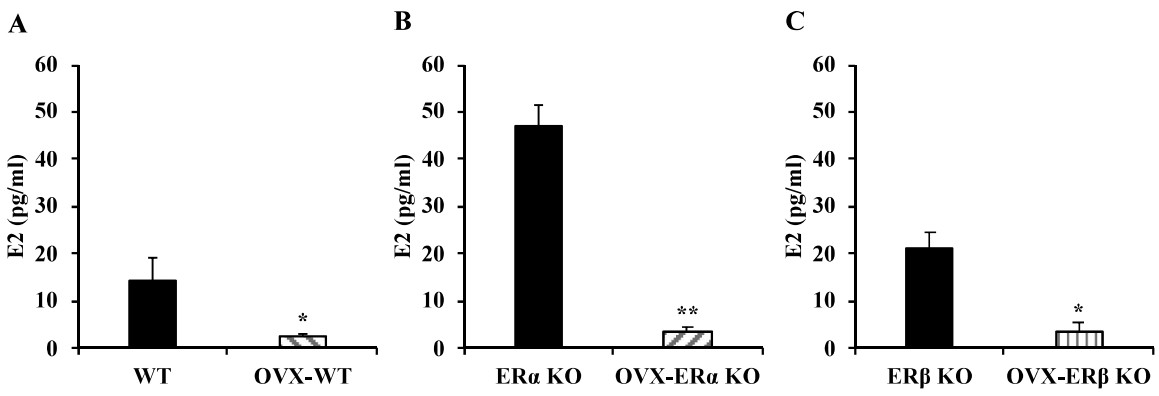


Fig. 9. E2 concentration in serum before and after OVX treatment of all three types of mice. E2 concentration in WT, ERα KO and ERβ KO mice (A, B, C). Data were shown as average ± SD, n = 3/groups, * and ** indicate significant difference between group before and after OVX treatment, $p < 0.05$ and $p < 0.01$, respectively, Student's *t*-test, two-tailed.

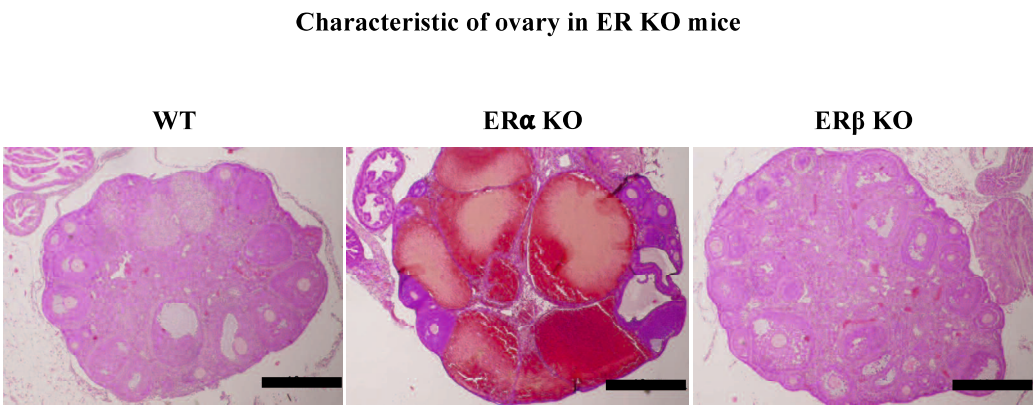


Fig. 10. Morphological changes of the ovary in ERα KO and ERβ KO mice compared with WT mice. Scale bar = 1 mm.

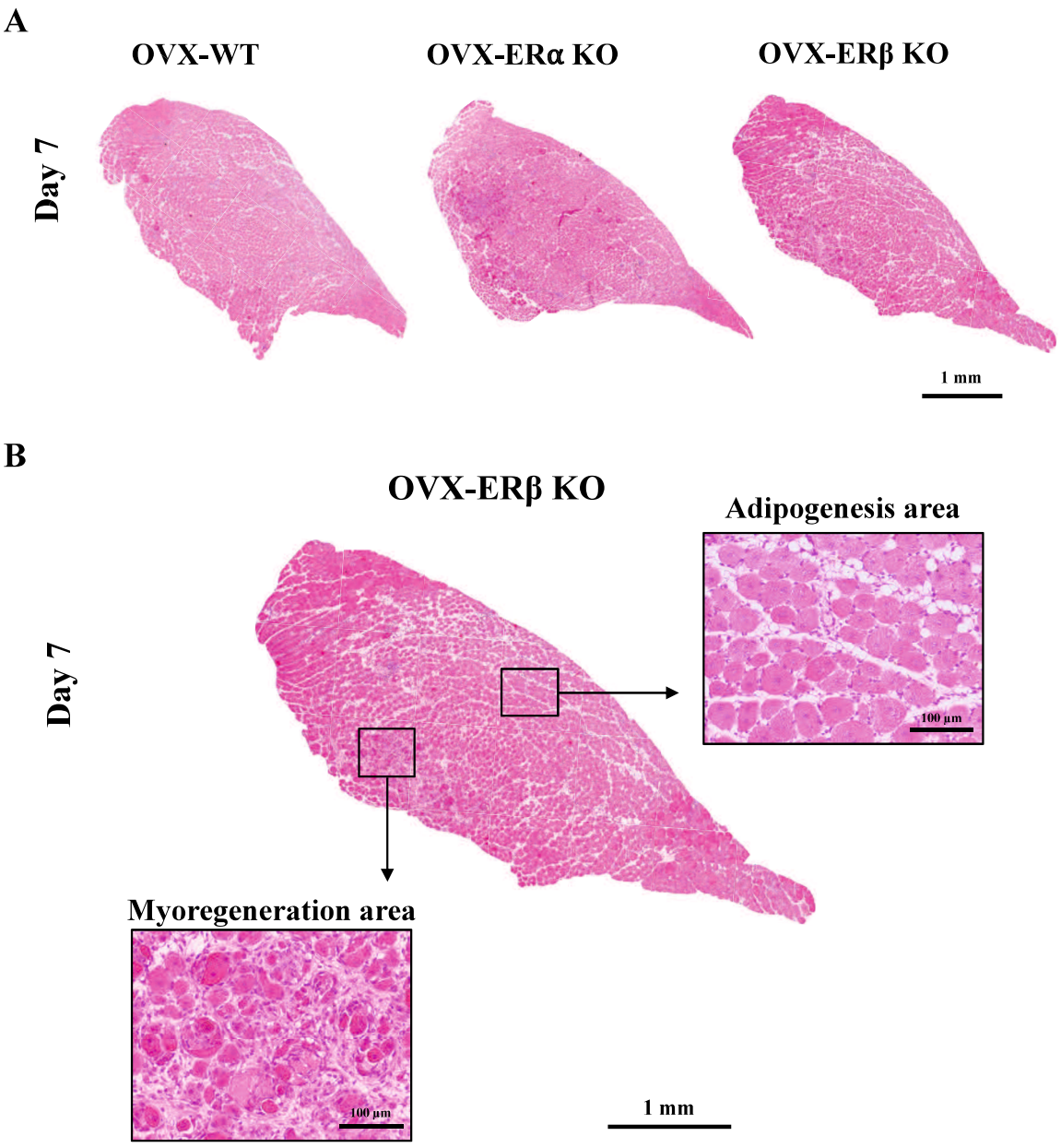


Fig. 11. Transverse sections of TA muscle. (A) Sections of TA muscle injected with CTX in OVX-WT mice as control, OVX-ERα KO and OVX-ERβ KO at D7 post CTX injection. (B) Myoregeneration and adipogenesis area of TA muscle section in OVX- ERβ KO mice at D7 post CTX injection.

A

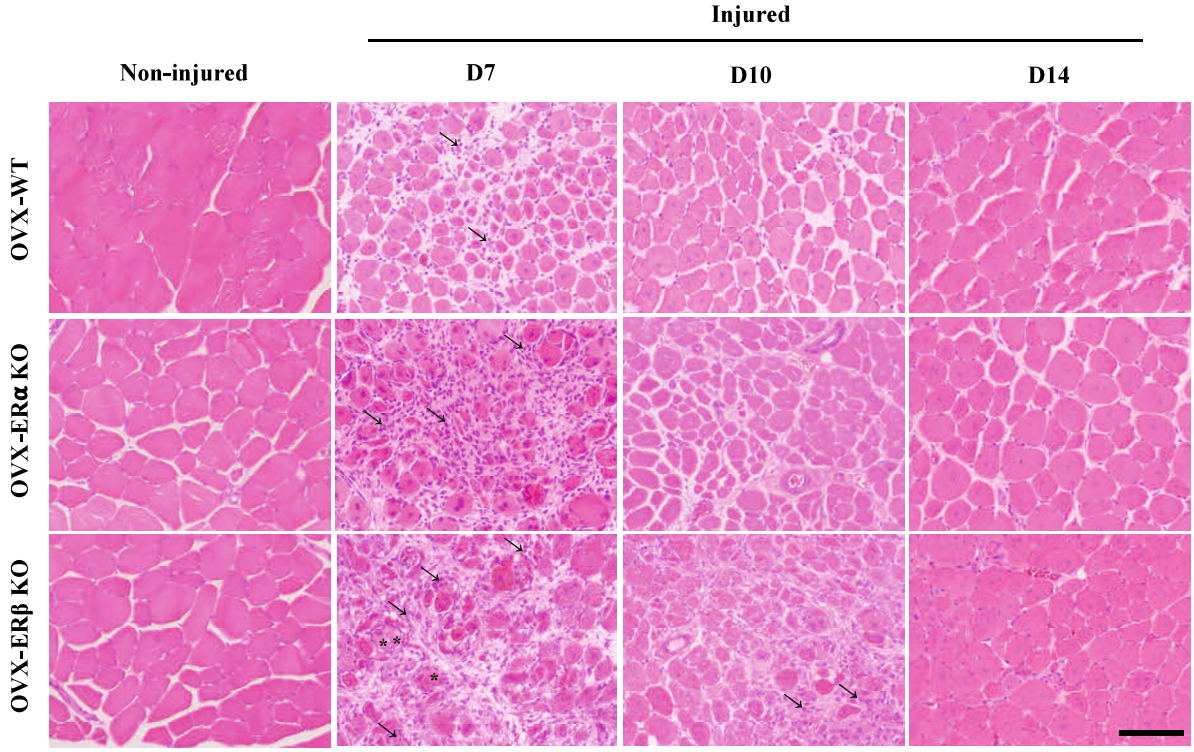
Injured
Non-injured
D7
D10
D14
OVX-WT
OVX-ERα KO
OVX-ERβ KO

B

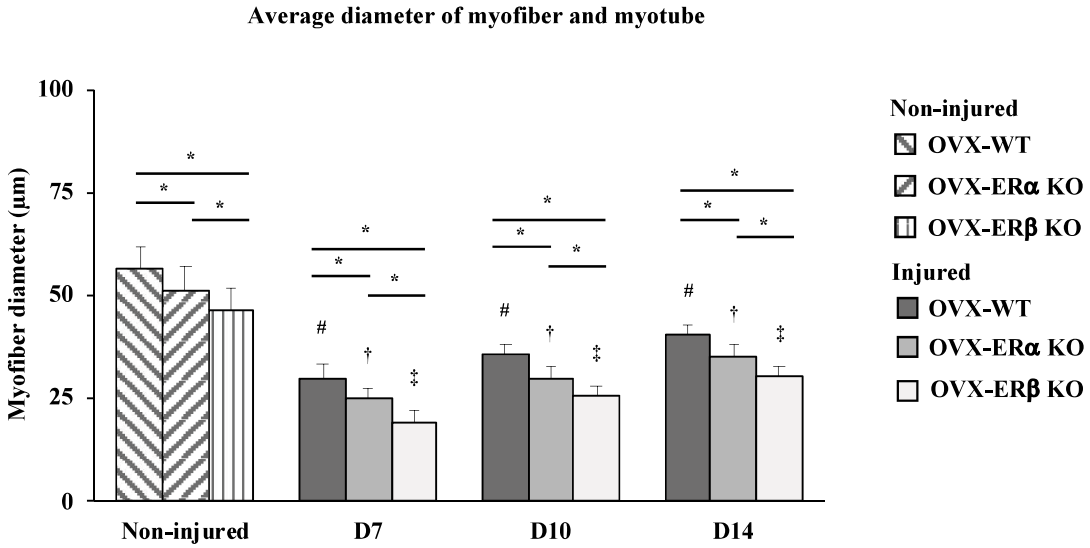
Average diameter of myofiber and myotube
Myofiber diameter (μm)
100
75
50
25
0
Non-injured
D7
D10
D14
Non-injured
OVX-WT
OVX-ERα KO
OVX-ERβ KO
Injured
OVX-WT
OVX-ERα KO
OVX-ERβ KO

Fig. 12. Regeneration of muscle in OVX treated WT, ERα KO and ERβ KO mice by CTX injection. (A) Sections of the TA muscle of non-injured control of OVX-WT mice, OVX-ERα KO and OVX-ERβ KO. Sections of the TA muscle injected with CTX at D7, D10 and D14 post injection. Arrows indicate cell infiltration among regenerated myofibers. Asterisks indicate necrotic myofibers. (B) Comparison of non-injured myofiber diameter and newly formed myofiber diameter at D7, D10 and D14 post CTX injection. Data are expressed as average ± SD, #, † and ‡ indicate significant differences from non-injured control in OVX-WT mice, OVX-ERα KO mice and OVX-ERβ KO mice, respectively ($p < 0.01$), * indicates significant difference between groups at time post injury, $p < 0.01$. Scale bar = 100 μm.

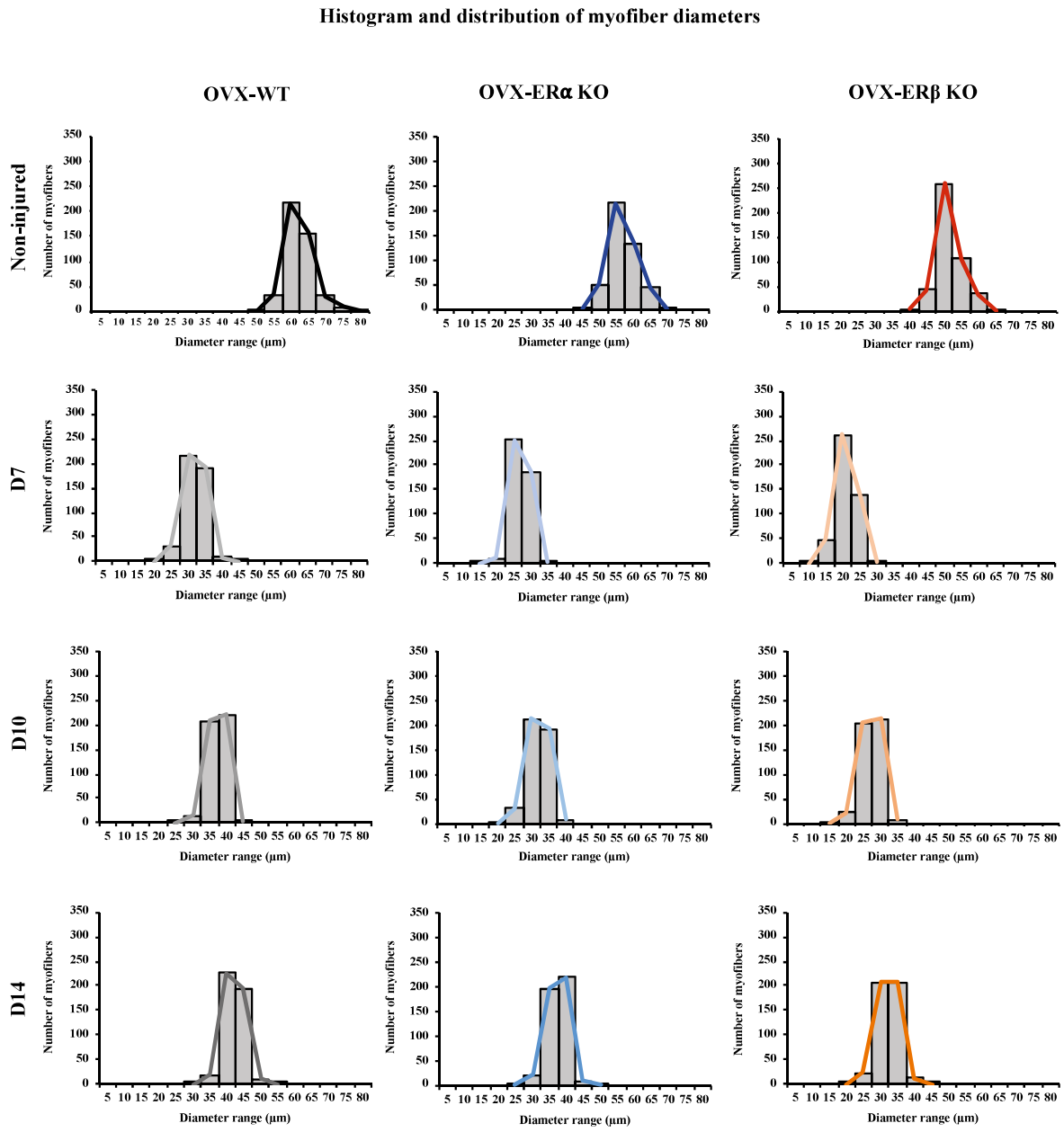


Fig. 13. The histogram and distribution line of myofiber and myotube diameters of non-injured control in OVX-WT, OVX-ERα KO and OVX-ERβ KO mice and at D7, D10 and D14 after CTX injection.

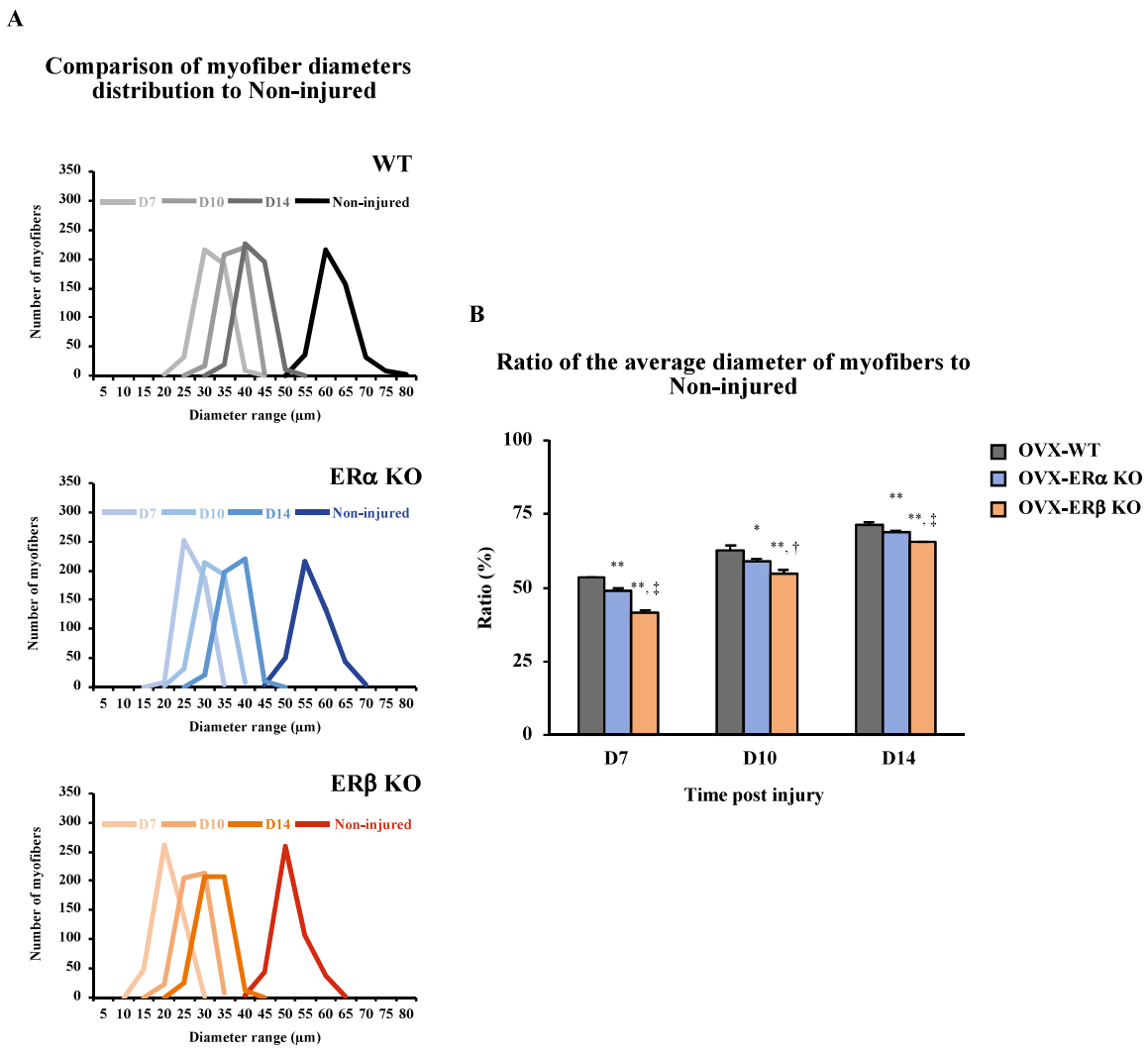


Fig. 14. (A) Comparative of the distribution diameter of myofiber and myotube diameters to non-injured in three types of mice (B) Ratio (%) of the average diameter of muscle fibers in each group to the average diameter of non-injured control at each time point. Average ratio percentage values of each group were compared using the Bonferroni/Dunn *post-hoc* tests. Average ± SD; n = 3. * $p < 0.05$, ** $p < 0.01$ vs. OVX-WT, respectively, † $p < 0.05$, ‡ $p < 0.01$ vs. OVX-ERα KO, respectively.

A

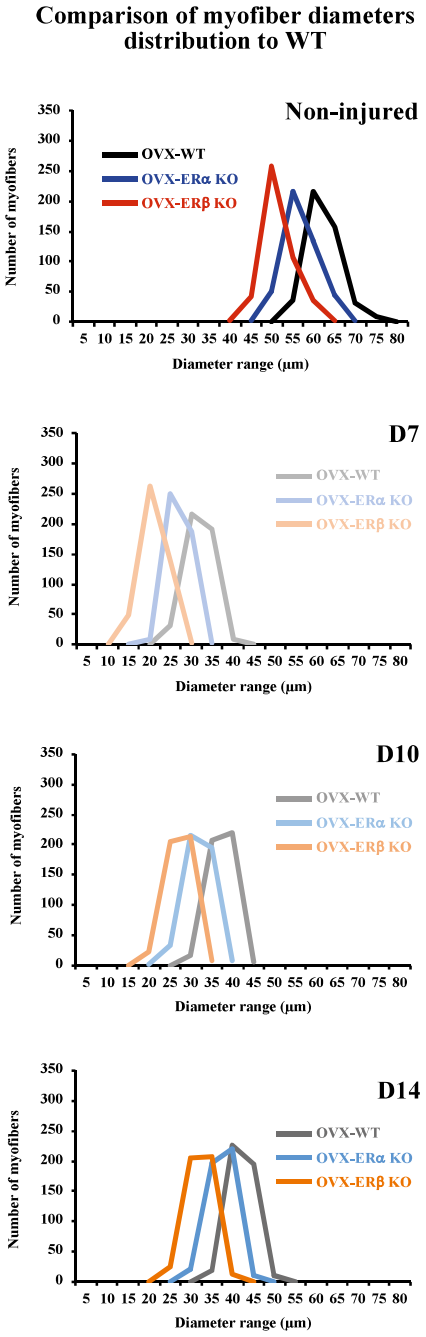
Comparison of myofiber diameters distribution to WT
Non-injured
OVX-WT
OVX-ERα KO
OVX-ERβ KO
Number of myofibers
Diameter range (µm)
D7
D10
D14

B

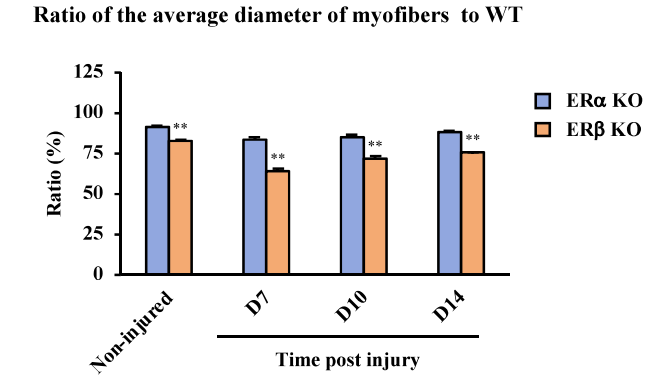
Ratio of the average diameter of myofibers to WT
ERα KO
ERβ KO
Ratio (%)
Non-injured
D7
D10
D14
Time post injury

Fig. 15. (A) Comparative of the distribution diameter of myofiber and myotube diameters to WT mice at non-injured and each time point after CTX injection. (B) Ratio (%) of the average diameter of muscle fibers in each group to the average diameter of WT at each time point. Data were shown as average ratio percentage ± SD. ** indicates significant difference from ERα KO mice, $p < 0.01$.

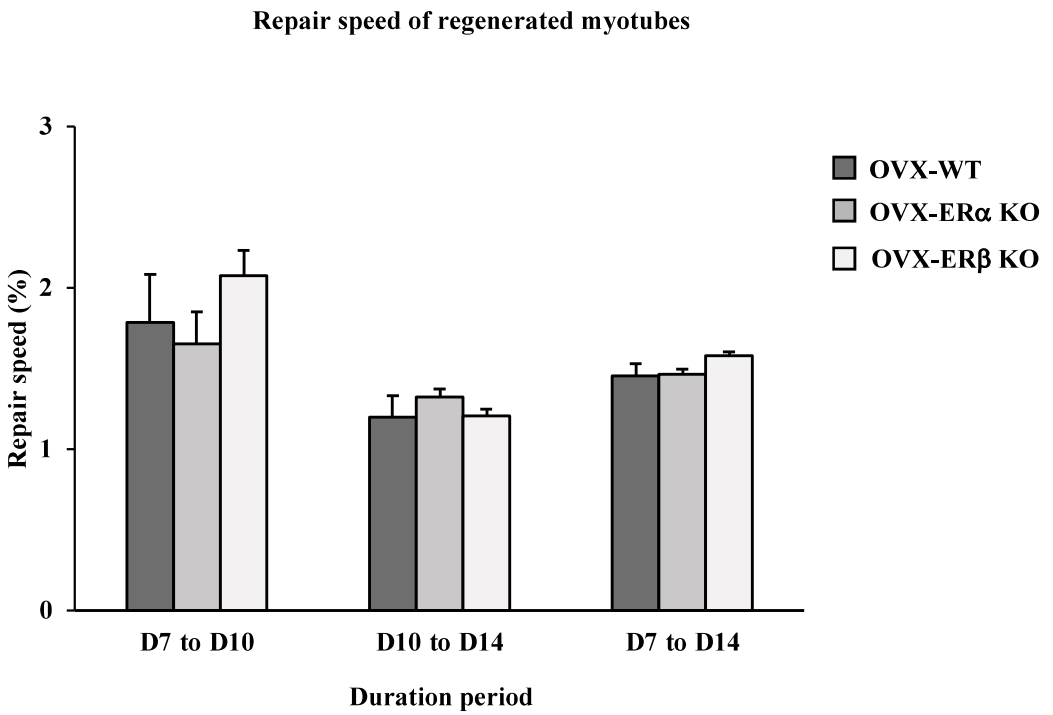


Fig. 16. Repair speed of regenerated muscle fibers in each group at several duration periods of days after injury (μm/day). Data were shown as average/day ± SD.

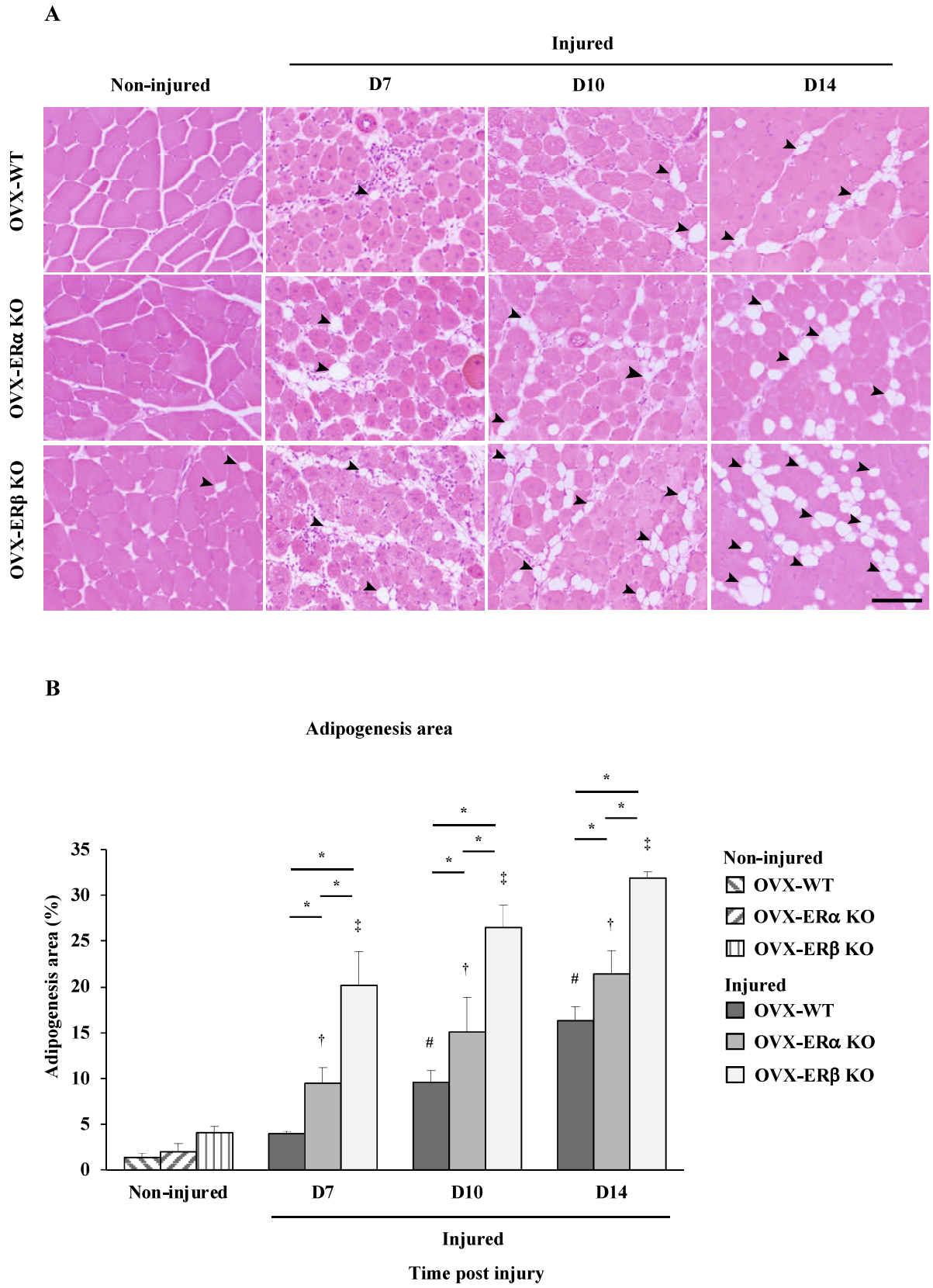
A
Injured
Non-injured
D7
D10
D14
OVX-WT
OVX-ERα KO
OVX-ERβ KO
B
Adipogenesis area
Adipogenesis area (%)
35
30
25
20
15
10
5
0
Non-injured
D7
D10
D14
Injured
Time post injury
Non-injured
OVX-WT
OVX-ERα KO
OVX-ERβ KO
Injured
OVX-WT
OVX-ERα KO
OVX-ERβ KO

Fig. 17. Intermuscular adipogenesis in OVX treated WT, ERα KO and ERβ KO mice after CTX injection. (A) Sections of the non-injured TA muscle of OVX-WT mice, OVX-ERα KO mice and OVX-ERβ KO mice. Sections of the TA muscle injected with CTX in OVX-WT mice, OVX-ERα KO mice and OVX-ERβ KO mice at D7, D10 and D14 post injection. Arrow heads indicate adipocytes among non-injured myofibers and regenerated myofibers. (B) Adipogenesis area (%) of all three types of non-injured OVX mice and OVX mice injected CTX at D7, D10 and D14 post injection. Data are expressed as average ± SD, #, † and ‡ indicate significant differences from non-injured control in OVX-WT mice, OVX-ERα KO mice and OVX-ERβ KO mice, respectively ($p < 0.05$). * indicates significant difference between groups at time post injury, $p < 0.05$. Scale bar = 100 μm.

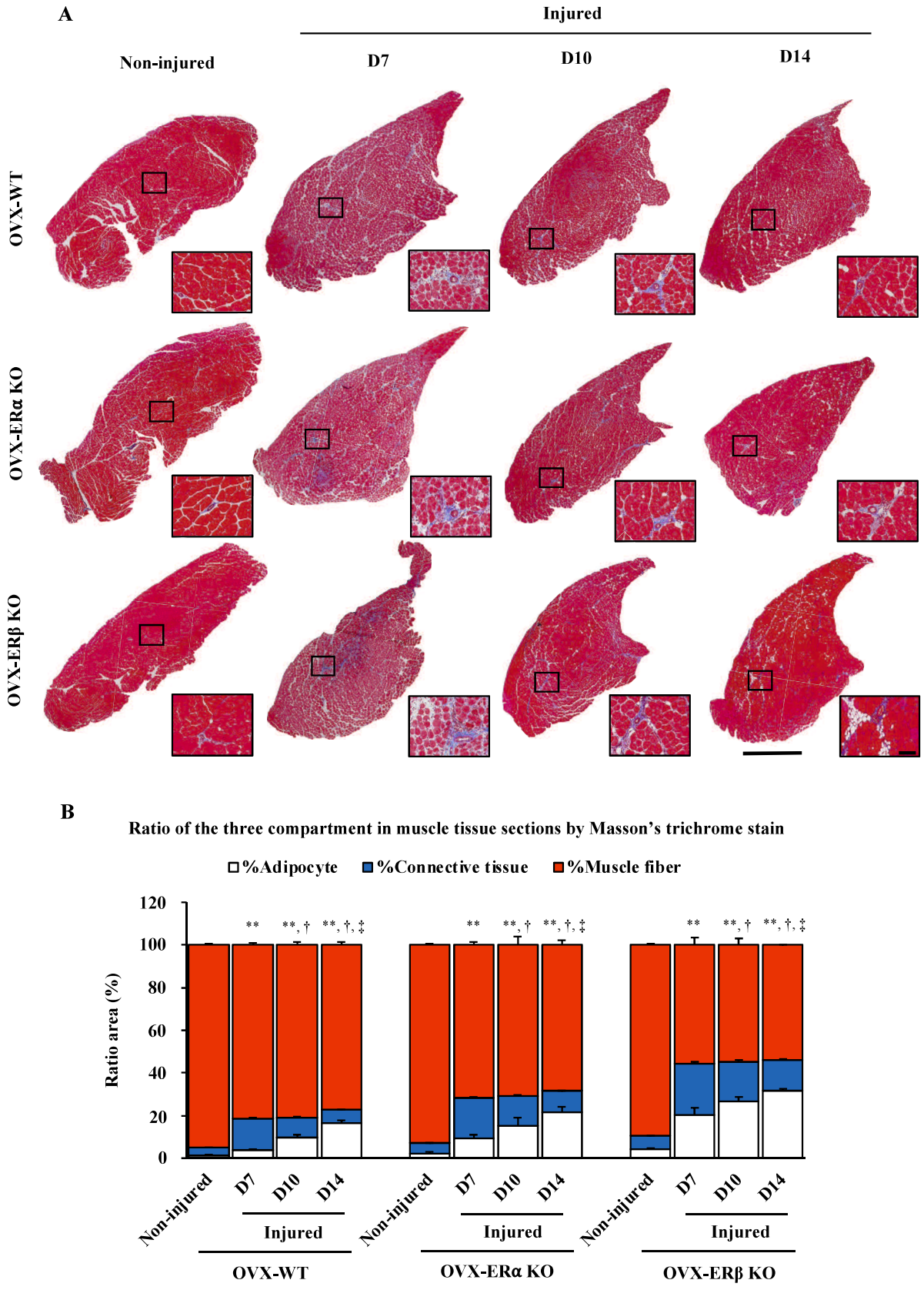
A
Injured
Non-injured
D7
D10
D14
OVX-WT
OVX-ERα KO
OVX-ERβ KO
B
Ratio of the three compartment in muscle tissue sections by Masson's trichrome stain
%Adipocyte
%Connective tissue
%Muscle fiber
Ratio area (%)
120
100
80
60
40
20
0
**
**, †
**, †, ‡
Non-injured
D7
D10
D14
Injured
OVX-WT
OVX-ERα KO
OVX-ERβ KO

Fig. 18. Masson's trichrome stain. (A) Sections of TA muscle injected with CTX and without CTX (non-injured as control) in OVX-WT mice, OVX-ERα KO mice and OVX-ERβ KO mice all time post CTX injection at D7, D10 and D14. Square areas within low magnification of whole section images are magnified in the right bottom panels. (B) Ratio of the three compartments in muscle tissue sections by Masson's trichrome stain. Myofiber area (red), adipocyte area (white), and connective tissue area (blue) (%) of all three types of non-injured OVX mice and OVX mice injected CTX at several time points post injection at D7, D10 and D14. Data are expressed as average ± SD. **, † and ‡ indicate significant differences from non-injured control of connective tissue area, D7 of connective tissue area and D10 of connective tissue area, respectively ($p < 0.01$). Scale bar = 1 mm (low magnification), 100 μm (high magnification).

## GENERAL SUMMARY

The content of this thesis adds significant and novel finding to the field of estrogen and estrogen receptors in myoregeneration and intermuscular adipogenesis. During the time of menopause, women loss of ovarian hormone, especially estrogen (E2: 17β-estradiol). Prior to my studies, the function of estrogen and estrogen receptors in myoregeneration was unclear. My studies have been little research completed *in vivo* to which estrogen receptor utilizes during myoregeneration process. Moreover, adipocytes increased between myofibers after tissue damage, but the area of adipocytes formed varied significantly between ERα KO mice and ERβ KO mice.

In Chapter 1, the diameters of regenerated myotubes in OVX mice after CTX injection were significantly smaller than those in intact mice after CTX injection. Most of the satellite cells, which play an important role in the myoregeneration process, remain in a quiescent status in healthy or uninjured muscle tissue. However, the muscle injury caused by mechanical loading or chemical injection activates satellite cells from a quiescent state to a state of proliferation, leading to the myoregeneration process. The results strongly suggest that muscle injury in a low estrogen status induces satellite cell loss, followed by delayed differentiation into myoblasts, resulting in delayed myoregeneration. Protein levels of the two ERs (ERα and ERβ) in TA muscles of mice showed a predominance of ERβ over ERα in both intact and OVX mouse samples. In this experiment, injection of CTX into OVX mice significantly increased ERβ production at D7, followed by a gradual decrease while maintaining high levels compared to those in OVX mice. Serum E2 levels increase in the early stages of trauma in adult human patients. This phenomenon suggests that estrogen may play an important role in the protection of traumatic organs. It is considered that the expression of ERβ in injured muscle tissue was upregulated to maintain the signal input from E2, which has a strong impact on

myoregeneration. Moreover, the investigation in the effect of a low E2 status on muscle recovery. The result suggests that estrogen is an essential factor for rescue of muscle recovery in a low E2 status. Being consistent with the results of that study, the diameter of regenerated myotubes in CTX-injured mice continuously treated with estrogen was significantly larger than that in OVX/CTX mice. It can be said that estrogen is a factor that acts when satellite cells are in a proliferated or differentiated state after muscle damage.

In Chapter 2, the both subtypes of OVX-ER KO mice after muscle injury by CTX injection, myofiber diameter was significantly low when comparing with OVX-WT mice. Satellite cells are stem cells of myofibers, and their initial cell growth is important for muscle regeneration smoothly. If satellite cell survival and proliferation were inhibited due to low estrogen status, this experiment may imply that the low number of satellite cells at early stages reflects the delay of myoregeneration. The myofiber diameter was significantly smaller in ERβ KO mice than in ERα KO mice. Based on these results, it can be inferred that the action of estrogen *via* ERβ has a stronger effect on the maintenance of muscle tissue homeostasis than ERα. Taken together, ERβ is likely to play a more important role in regulating myoregeneration than ERα in muscle tissue. Delay of myoregeneration and induction of intermuscular adipogenesis in CTX-injured OVX-ER KO mice may alter the muscle and fat metabolism pathways and alter gene expression in muscle tissue. PDGFRα are the origin of intermuscular adipocytes. In this experiment, adipocytes increased between myofibers after tissue damage, but the area of adipocytes formed varied significantly between ERα KO mice and ERβ KO mice. It is easy to imagine that the number and proliferation of PDGFRα-positive mesenchymal progenitor cells have a great influence on the proliferation of adipocytes after muscle tissue damage. In sarcopenia, accumulation of ectopic adipose tissue is observed in skeletal muscle, as well as atrophy of myofibers and deterioration of muscle strength and physical function.

Comparing the CTX-injured and sarcopenic muscle, there are many morphologically similar parts.

In conclusion, the data presented in this thesis provided evidence that estrogen is an essential factor for the maintenance of satellite cell proliferation and differentiation in the smooth progression of myoregeneration. Further elucidation of the mechanism of the myoregeneration process will enable the establishment of new strategies for maintaining female muscle function by targeting the estrogen-ER pathway. The low estrogen affects myoregeneration *via* the ER. Its action was more remarkable *via* ERβ rather than by ERα, and it was morphologically shown that removal of these ERs delayed muscle regeneration and promoted adipose tissue formation.

## ACKNOWLEDGEMENTS

First of all, I would like to show the greatest appreciation to Professor Dr. Yoshinao Hosaka, Tottori University, for his kindness support throughout my student life in Japan. He taught me to understand a scientific attitude and to carry out the scientific experiments. I have learnt numerous scientific techniques from him. Here is a special thanks from my heart to him for his elaborated guidance, kindness encouragement, and invaluable suggestion. Everything that he taught me leads me understand how to be a good researcher, a great professor and an excellent leader.

Besides, a special thanks to Associate Prof. Dr. Katsuhiko Warita and Professor Dr. Akira Yabuki, my co-supervisor from Tottori University and Kagoshima University, respectively. Also, I am indebted to all students from Laboratory of Veterinary Anatomy, Tottori University for their contributions had indeed supported my work.

I would like to thank for Associate Prof. Dr. Bongkot Noppon (Emeritus, Khon Kaen University, Thailand), Associate Prof. Dr. Prasarn Tangkawattana (Khon Kaen University, Thailand) and Associate Prof. Dr. Worapol Aengwanich (Mahasarakham University, Thailand) for guiding me during my first step of scientific research as well as for giving me precious advice on the personal level.

Furthermore, my deepest gratitude to Ministry of Education, Culture, Sports, Science and Technology, Japan for the generous scholarship and the opportunity to pursue the doctoral degree in Japan. I also would like to tender my greatest appreciation to the United Graduate School of Veterinary Science, Yamaguchi University for the support and the sponsorships to attend international and national veterinary conferences.

Finally, I dedicate this thesis to my wife for her constant support and unconditional love throughout this entire academic endeavor. She has always told me to strive for greatness and that nothing was impossible. She gaves me everything I needed to succeed in life and I am forever grateful for all she has sacrificed for my dreams.

## REFERENCES


Adams, G. R. and McCue S. A. 1998. Localized infusion of IGF-I results in skeletal muscle hypertrophy in rats. *J. Appl. Physiol.* **84**: 1716–1722.

Baltgalvis, K. A., Greising, S. M., Warren, G. L. and Lowe, D. A. 2010. Estrogen regulates estrogen receptors and antioxidant gene expression in mouse skeletal muscle. *PLoS One* 5: e10164.

Brown, M. 2008. Skeletal muscle and bone: effect of sex steroids and aging. *Adv. Physiol. Educ.* **32**: 120–126.

Brown, C. M., Suzuki, S., Jelks, K. A. and Wise, P. M. 2009. Estradiol is a potent protective, restorative, and trophic factor after brain injury. *Semin. Reprod. Med.* **27**: 240–249.

Brown, M., Ning, J., Ferreira, J. A., Bogener, J. L. and Lubahn, D. B. 2009. Estrogen receptor-α and -β and aromatase knockout effects on lower limb muscle mass and contractile function in female mice. *Am. J. Physiol. Endocrinol. Metab.* **296**: 854–861.

Campbell, S. E. and Febbraio, M. A. 2001. Effect of ovarian hormones on mitochondrial enzyme activity in the fat oxidation pathway of skeletal muscle. *Am. J. Physiol. Endocrinol. Metab.* **281**: 803–808.

Chargé, S. B. and Rudnicki, M. A. 2004. Cellular and molecular regulation of muscle regeneration. *Physiol. Rev.* **84**: 209–238.

Chen, R, S., Zhang, X, B., Zhu, X, T. and Wang, C, S. 2020. The crosstalk between IGF-1R and ER-α in the proliferation and anti-inflammation of nucleus pulposus cells. *Eur. Rev. Med. Pharmacol. Sci.* **24**: 5886–5894.

Chidi-Ogbolu, N. and Baar, K. 2019. Effect of estrogen on musculoskeletal performance and injury risk. *Front. Physiol.* 9: 1834.

Collins, B. C., Arpke, R. W., Larson, A. A., Baumann, C. W., Xie, N., Cabelka, C. A., Nash, N. L., Juppi, H. K., Laakkonen, E. K., Sipilä, S., Kovanen, V., Spangenburg, E. E., Kyba, M. and Lowe, D. A. 2019. Estrogen regulates the satellite cell compartment in females. *Cell Rep.* **28**: 368–381.

Contreras-Shannon, V., Ochoa, O., Reyes-Reyna, S. M., Sun, D., Michalek, J. E., Kuziel, W. A., McManus, L. M. and Shireman, P. K. 2006. Fat accumulation with altered inflammation and regeneration in skeletal muscle of CCR2$^{-/-}$ mice following ischemic injury. *Am. J. Physiol. Cell Physiol.* **292**: 953–967.

Deng, B., Zhang, F., Wen, J., Ye, S., Wang, L., Yang, Y., Gong, P. and Jiang, S. 2017. The function of myostatin in the regulation of fat mass in mammals. *Nutr. Metab. (Lond).* **21**: 14–29.

Diel, P. 2014. The role of the estrogen receptor in skeletal muscle mass homeostasis and regeneration. *Acta Physiol. (Oxf).* **212**: 14–16.

Dupont, S., Krust, A., Gansmuller, A., Dierich, A., Chambon, P. and Mark, M. 2000. Effect of single and compound knockouts of estrogen receptors α (ERα) and β (ERβ) on mouse reproductive phenotypes. *Development* **127**: 4277–4291.

Ekenros, L., Papoutsi, Z., Fridén, C., Dahlman Wright, K. and Lindén Hirschberg, A. 2017. Expression of sex steroid hormone receptors in human skeletal muscle during the menstrual cycle. *Acta Physiol. (Oxf).* **219**: 486–493.

Enns, D. L. and Tiidus, P. M. 2008. Estrogen influences satellite cell activation and proliferation following downhill running in rats. *J. Appl. Physiol.* **104**: 347–353.

Forcina, L., Cosentino, M. and Musarò, A. 2020. Mechanisms regulating muscle regeneration: insights into the interrelated and time-dependent phases of tissue healing. *Cells* 9: 1297.

Galluzzo, P., Rastelli, C., Bulzomi, P., Acconcia, F., Pallottini, V. and Marino, M. 2009. 17β-estradiol regulates the first steps of skeletal muscle cell differentiation via ER-α-mediated signals. *Am. J. Physiol. Cell Physiol.* **297**: 1249–1262.

Geraci, A., Calvani, R., Ferri, E., Marzetti, E., Arosio, B. and Cesari, M. 2021. Sarcopenia and menopause: the role of estradiol. *Front. Endocrinol. (Lausanne)* 12: 682012.

Girousse, A., Gil-Ortega, M., Bourlier, V., Bergeaud, C., Sastourné-Arrey, Q., Moro, C., Barreau, C., Guissard, C., Vion, J., Arnaud, E., Pradère, J. P., Juin, N., Casteilla, L. and Sengenès, C. 2019. The release of adipose stromal cells from subcutaneous adipose tissue regulates ectopic intramuscular adipocyte deposition. *Cell Rep*. **27**: 323–333

Gorres, B. K., Bomhoff, G. L., Gupte, A. A. and Geiger, P. C. 2011. Altered estrogen receptor expression in skeletal muscle and adipose tissue of female rats fed a high-fat diet. *J. Appl. Physiol.* **110**: 1046–1053.

Greising, S. M., Baltgalvis, K. A., Kosir, A. M., Moran, A. L., Warren, G. L. and Lowe, D. A. 2011. Estradiol's beneficial effect on murine muscle function is independent of muscle activity. *J. Appl. Physiol.* **110**: 109–115.

Greising, S. M., Baltgalvis, K. A., Lowe, D. A. and Warren, G. L. 2009. Hormone therapy and skeletal muscle strength: a meta-analysis. *J. Gerontol. A. Biol. Sci. Med. Sci.* **64**: 1071–1081.

Groswasser, Z. 2001. Gender and traumatic brain injury. *J. Neurosurg.* **94**: 862–864.

Haines, M., McKinley-Barnard, S. K., Andre, T. L., Gann, J. J., Hwang, P. S. and Willoughby, D. S. 2018. Skeletal muscle estrogen receptor activation in response to eccentric exercise up-regulates myogenic-related gene expression independent of differing serum estradiol levels occurring during the human menstrual cycle. *J. Sport Sci. Med.* **17**: 31–39.

Hausman, G. J., Basu, U., Du, M., Fernyhough-Culver, M. and Dodson, M. V. 2014. Intermuscular and intramuscular adipose tissues: bad vs. good adipose tissues. *Adipocyte* **10**: 242–255.

Hewitt, S. C., Couse, J. F. and Korach, K. S. 2000. Estrogen receptor transcription and transactivation estrogen receptor knockout mice: what their phenotypes reveal about mechanisms of estrogen action. *Breast Cancer Res.* **2**: 345–352.

Iida, M., Tsuboi, K., Niwa, T., Ishida, T. and Hayashi, S. I. 2019. Compensatory role of insulin-like growth factor 1 receptor in estrogen receptor signaling pathway and possible therapeutic target for hormone therapy-resistant breast cancer. *Breast Cancer* **26**: 272–281.

Ikeda, K., Horie-Inoue, K. and Inoue, S. 2019. Functions of estrogen and estrogen receptor signaling on skeletal muscle. *J. Steroid Biochem. Mol. Biol.* 191: 105375.

Jackson, K. C., Wohlers, L. M., Lovering, R. M., Schuh, R. A., Maher, A. C., Bonen, A., Koves, T. R., Ilkayeva, O., Thomson, D. M., Muoio, D. M. and Spangenburg, E. E. 2013. Ectopic lipid deposition and the metabolic profile of skeletal muscle in ovariectomized mice. *Am. J. Physiol. Regul. Integr. Comp. Physiol.* **304**: 206–217.

Kalbe, C., Mau, M., Wollenhaupt, K. and Rehfeldt, C. 2007. Evidence for estrogen receptor α and β expression in skeletal muscle of pigs. *Histochem. Cell Biol.* **127**: 95–107.

Karalaki, M., Fili, S., Philippou, A. and Koutsilieris, M. 2009. Muscle regeneration: cellular and molecular events. *In Vivo* **23**: 779–796.

Kawai, S., Takagi, Y., Kaneko, S. and Kurosawa, T. 2011. Effect of three types of mixed anesthetic agents alternate to ketamine in mice. *Exp. Anim.* **60**: 481–487.

Kiens, B. 2006. Skeletal muscle lipid metabolism in exercise and insulin resistance. *Physiol. Rev.* **86**: 205–243.

Kitajima, Y. and Ono, Y. 2016. Estrogens maintain skeletal muscle and satellite cell functions. *J. Endocrinol.* **229**: 267–275.

Koike, T., Mikami, T., Shida, M., Habuchi, O. and Kitagawa, H. 2015. Chondroitin sulfate-E mediates estrogen-induced osteoanabolism. *Sci. Rep.* 5: 8994.

Kosir, A. M., Mader, T. L., Greising, A. G., Novotny, S. A., Baltgalvis, K. A. and Lowe, D. A. 2015. Influence of ovarian hormones on strength loss in healthy and dystrophic female mice. *Med. Sci. Sports Exerc.* **47**: 1177–1187.

Krege, J. H., Hodgin, J. B., Couse, J. F., Enmark, E., Warner, M., Mahler, J. F., Sar, M., Korach, K. S., Gustafsson, J. Å. and Smithies, O. 1998. Generation and reproductive phenotypes of mice lacking estrogen receptor β. *Proc. Natl. Acad. Sci. U S A.* **95**: 15677–15682.

LaBarge, S., McDonald, M., Smith-Powell, L., Auwerx, J. and Huss, J. M. 2014. Estrogen-related receptor-α (ERRα) deficiency in skeletal muscle impairs regeneration in response to injury. *FASEB. J.* **28**: 1082–1097.

La Colla, A., Pronsato, L., Milanesi, L. and Vasconsuelo, A. 2015. 17β-estradiol and testosterone in sarcopenia: Role of satellite cells. *Ageing Res. Rev.* **24**: 166–177.

Le, G., Novotny, S. A., Mader, T. L., Greising, S. M., Chan, S. S. K., Kyba, M., Lowe, D. A. and Warren, G. L. 2018. A moderate oestradiol level enhances neutrophil number and activity in muscle after traumatic injury but strength recovery is accelerated. *J. Physiol.* **596**: 4665–4680.

Li, F., Yang, H., Duan, Y. and Yin, Y. 2011, Myostatin regulates preadipocyte differentiation and lipid metabolism of adipocyte via ERK1/2. *Cell Biol. Int.* **35**: 1141–1146.

Liao, Z. H., Huang, T., Xiao, J. W., Gu, R. C., Ouyang, J., Wu, G. and Liao, H. 2019. Estrogen signaling effects on muscle-specific immune responses through controlling the recruitment and function of macrophages and T cells. *Skelet. Muscle* 9: 20.

Luine, V. N., 2014. Estradiol and cognitive function: past, present and future. *Horm. Behav.* **66**: 602–618.

Mahdy, M. A., Lei, H. Y., Wakamatsu, J., Hosaka, Y. Z. and Nishimura, T. 2015. Comparative study of muscle regeneration following cardiotoxin and glycerol injury. *Ann. Anat.* **202**: 18–27.

Maher, A. C., Akhtar, M. and Tarnopolsky, M. A. 2010. Men supplemented with 17β-estradiol have increased β-oxidation capacity in skeletal muscle. *Physiol. Genomics* **42**: 342–347.

Mann, C. J., Perdiguero, E., Kharraz, Y., Aguilar, S., Pessina, P., Serrano, A. L. and Muñoz-Cánoves, P. 2011. Aberrant repair and fibrosis development in skeletal muscle. *Skelet. Muscle* 1: 21.

McClung, J. M., Davis, J. M., Wilson, M. A., Goldsmith, E. C. and Carson, J. A. 2006. Estrogen status and skeletal muscle recovery from disuse atrophy. *J. Appl. Physiol.* **100**: 2012–2023.

McCormick, K. M., Burns, K. L., Piccone, C. M., Gosselin, L. E. and Brazeau, G. A. 2004. Effects of ovariectomy and estrogen on skeletal muscle function in growing rats. *J. Muscle Res. Cell Motil.* **25**: 21–27.

McHale, M. J., Sarwar, Z. U., Cardenas, D. P., Porter, L., Salinas, A. S., Michalek, J. E., McManus, L. M. and Shireman, P. K. 2012. Increased fat deposition in injured skeletal muscle is regulated by sex-specific hormones. *Am. J. Physiol. Regul. Integr. Comp. Physiol.* **302**: 331–339.

McPherron, A. C. and Lee, S. J. 1997. Double muscling in cattle due to mutations in the myostatin gene. *Proc. Natl. Acad. Sci. U. S. A.* **94**: 12457–12461.

Messier, V., Rabasa-Lhoret, R., Barbat-Artigas, S., Elisha, B., Karelis, A. D. and Aubertin-Leheudre, M. 2011. Menopause and sarcopenia: A potential role for sex hormones. *Maturitas* **68**: 331–336.

Milanesi, L., Russo de Boland, A. and Boland, R. 2008. Expression and localization of estrogen receptor alpha in the C2C12 murine skeletal muscle cell line. *J. Cell. Biochem.* **104**: 1254–1273.

Milanesi, L., Vasconsuelo, A., de Boland, A. R. and Boland, R. 2009. Expression and subcellular distribution of native estrogen receptor beta in murine C2C12 cells and skeletal muscle tissue. *Steroids* **74**: 489–497.

Muramatsu, M. and Inoue, S. 2000. Estrogen receptors: how do they control reproductive and nonreproductive functions? *Biochem. Biophys. Res. Commun.* **270**: 1–10.

Nagai, S., Ikeda, K., Horie-Inoue, K., Shiba, S., Nagasawa, S., Takeda, S. and Inoue, S. 2016. Estrogen modulates exercise endurance along with mitochondrial uncoupling protein 3 downregulation in skeletal muscle of female mice. *Biochem. Biophys. Res. Commun.* **480**: 758–764.

Nagai, S., Ikeda, K., Horie–Inoue, K., Takeda, S. and Inoue, S. 2018. Estrogen signaling increases nuclear receptor subfamily 4 group A member 1 expression and energy production in skeletal muscle cells. *Endocr. J.* **65**: 1209–1218.

Nelson, L. R. and Bulun, S. E. 2001. Estrogen production and action. *J. Am. Acad. Dermatol.* **45**: 116–124.

Nilsson, S. and Gustafsson, J. Å. 2011. Estrogen receptors: therapies targeted to receptor subtypes. *Clin. Pharmacol. Ther.* **89**: 44–55.

Ochoa, O., Sun, D., Reyes-Reyna, S. M., Waite, L. L., Michalek, J. E., McManus, L. M. and Shireman, P. K. 2007. Delayed angiogenesis and VEGF production in CCR2-/- mice during impaired skeletal muscle regeneration. *Am. J. Physiol. Regul. Integr. Comp. Physiol.* **293**: 651–661.

Pöllänen, E., Sipilä, S., Alen, M., Ronkainen, P. H., Ankarberg-Lindgren, C., Puolakka, J., Suominen, H., Hämäläinen, E., Turpeinen, U., Konttinen, Y. T. and Kovanen, V. 2011.

Differential influence of peripheral and systemic sex steroids on skeletal muscle quality in pre- and postmenopausal women. *Aging Cell* **10**: 650–660.

Relaix, F. and Zammit, P. S. 2012. Satellite cells are essential for skeletal muscle regeneration: the cell on the edge returns centre stage. *Development* **139**: 2845–2856.

Schmidt, M., Schüler, S. C., Hüttner, S. S., von Eyss, B. and von Maltzahn, J. 2019. Adult stem cells at work: regenerating skeletal muscle. *Cell. Mol. Life Sci.* **76**: 2559–2570.

Seko, D., Fujita, R., Kitajima, Y., Nakamura, K., Imai, Y. and Ono, Y. 2020. Estrogen receptor β controls muscle growth and regeneration in young female mice. *Stem Cell Reports* **15**: 577–586.

Seo, K., Suzuki, T., Kobayashi., K. and Nishimura, T. 2019. Adipocytes suppress differentiation of muscle cells in a co-culture system. *Anim. Sci. J.* **90**: 423–434.

Srikanthan, P., Hevener, A. L. and Karlamangla, A. S. 2010. Sarcopenia exacerbates obesity-associated insulin resistance and dysglycemia: findings from the national health and nutrition examination survey III. *PLoS One* 5: e10805.

Sun, W. X., Dodson, M. V., Jiang, Z. H., Yu, S. G., Chu, W. W. and Chen, J. 2016. Myostatin inhibits porcine intramuscular preadipocyte differentiation in vitro. *Domest. Anim. Endocrinol.* **55**: 25–31.

Tang, H., Liao, Y., Chen, G., Xu, L., Zhang, C., Ju, S. and Zhou, S. 2012. Estrogen upregulates the IGF-1 signaling pathway in lung cancer through estrogen receptor-β. *Med. Oncol.* **29**: 2640–2648.

Tidball, J. G. 2017. Regulation of muscle growth and regeneration by the immune system. *Nat. Rev. Immunol.* **17**: 165–178.

Tiidus, P. M., Lowe, D. A. and Brown, M. 2013. Estrogen replacement and skeletal muscle: mechanisms and population health. *J. Appl. Physiol.* **115**: 569–578.

Tsai, W. J., McCormick, K. M., Brazeau, D. A. and Brazeau, G. A. 2007. Estrogen effects on skeletal muscle insulin-like growth factor 1 and myostatin in ovariectomized rats. *Exp. Biol. Med. (Maywood).* **232**: 1314–1325.

Uezumi, A., Fukada, S., Yamamoto, N., Takeda, S. and Tsuchida, K. 2010. Mesenchymal progenitors distinct from satellite cells contribute to ectopic fat cell formation in skeletal muscle. *Nat. Cell Biol.* **12**: 143–152.

Velders, M., Schleipen, B., Fritzemeier, K. H., Zierau, O. and Diel, P. 2012. Selective estrogen receptor-β activation stimulates skeletal muscle growth and regeneration. *FASEB. J.* **26**: 1909–1920.

Wada, K., Katsuta, S. and Soya, H. 2008. Formation process and fate of the nuclear chain after injury in regenerated myofiber. *Anat. Rec. (Hoboken)* **291**: 122–128.